NASA Technical Paper 1915

Simulator Evaluation of Separation of Display Parameters in Path-Following Tasks

Garimella R. Sarma and James J. Adams

OCTOBER 1981

NASA

NASA Technical Paper 1915

Simulator Evaluation of Separation of Display Parameters in Path-Following Tasks

Garimella R. Sarma and James J. Adams
Langley Research Center
Hampton, Virginia

NASA
National Aeronautics
and Space Administration

Scientific and Technical
Information Branch

1981

SUMMARY

A fixed-base simulation study with five degrees of freedom was undertaken to examine the pilot's response to separation or integration of essential information in aircraft displays. The parameters displayed were bank angle, pitch angle, heading angle, and vertical- and lateral-displacement errors. The tasks of path following under turbulence and step-displacement correction were performed separately. Eight pilots with various amounts of experience participated in the study.

Analysis of the results shows that the accuracy of the lateral path-following task under turbulence deteriorates and the system damping reduces when bank angle is displayed separately, and the accuracy improves considerably when bank angle and heading are displayed together. No significant changes were observed in vertical control. The results show that displaying bank angle, pitch angle, and heading angle together in one place with displacements together in another location gives the best performance for all the configurations considered.

INTRODUCTION

In order to control the lateral and vertical displacements in an instrument landing system (ILS) approach to landing, the pilot must coordinate his response to bank angle, heading angle, and lateral displacements to obtain good lateral response, and he must coordinate pitch angle and vertical displacements to obtain good vertical response. The displays of these parameters are usually presented in several different locations on the instrument panel of a general aviation airplane. The bank angle and pitch angle are displayed in a two-axis gyro display, the heading angle in a directional gyro at a different location, and displacement errors at still another location. The pilot must scan these separated pieces of information for proper control. The scanning of the displays of these essential parameters must logically introduce an additional work load compared with a case for which all the information is presented together in a single display. In a recent investigation with conventional types of general aviation displays (ref. 1), it was found that instrument configurations can contribute to pilot-aircraft system instability, even though the aircraft are designed for good pilot-aircraft system stability. An earlier investigation reports a reduction in pilot gain and generation of more remnant when the displays are separated (ref. 2). The present study delineates the effects of separation or integration of parameter displays on aircraft control for path-following tasks. The effects are presented in terms of system performance, pilot models, and pilot-aircraft system closed-loop stability. A fixed-base simulation study with five degrees of freedom was used to obtain the data.

SYMBOLS

F_{y_p} side force due to rolling velocity, N-sec

F_{y_r} side force due to yawing velocity, N-sec

F_{y_β} side force due to sideslip, N

F_{z_α} vertical force due to angle of attack, N

g	acceleration due to gravity, m/sec^2
h	altitude, m
I_X, I_Y, I_Z	moments of inertia, $kg\text{-}m^2$
I_{XZ}	product of inertia, $kg\text{-}m^2$
K_h, K_y	pilot-model gains, rad/m
K_n	pilot-model remnant gain, dimensionless
K_θ, K_ψ, K_ϕ	pilot-model gains, dimensionless
m	mass of aircraft, kg
M_{X_p}	rolling moment due to roll velocity, N-m-sec
M_{X_r}	rolling moment due to yawing velocity, N-m-sec
M_{X_β}	rolling moment due to sideslip, N-m
$M_{X_{\delta_a}}$	rolling moment due to aileron deflection, N-m
M_{Y_α}	pitching moment due to angle of attack, N-m
M_{Y_q}	pitching moment due to pitch rate, N-m-sec
$M_{Y_{\delta_e}}$	pitching moment due to elevator deflection, N-m
M_{Z_p}	yawing moment due to rolling velocity, N-m-sec
M_{Z_r}	yawing moment due to yawing velocity, N-m-sec
M_{Z_β}	yawing moment due to sideslip, N-m
$M_{Z_{\delta_a}}$	yawing moment due to aileron deflection, N-m
P	probability that the scores are equal
p,q,r	roll, pitch, and yaw angular rates, rad/sec
s	Laplace operator, per second
T_R	aircraft roll time constant, sec
T_S	aircraft spiral time constant, sec
V	velocity, m/sec
y	lateral-displacement error, m
α,β	angles of attack and sideslip, rad

$\gamma_C, \gamma_{DR}, \gamma_y, \gamma_\phi$ system modes of motion

Δh altitude error, m

δ_a, δ_e aileron and elevator deflections, rad

ζ damping ratio

ψ, θ, ϕ heading, pitch, and bank angles, rad or deg

ω frequency, rad/sec

ω_C, ζ_C
ω_{DR}, ζ_{DR}
ω_h, ζ_h
ω_y, ζ_y
$\omega_\alpha, \zeta_\alpha$
ω_ϕ, ζ_ϕ

} frequencies, rad/sec, and damping ratios for pilot model-aircraft system modes of motion

ω_d damped natural frequency, rad/sec, $\omega_n\sqrt{1 - \zeta^2}$

ω_n natural frequency, rad/sec

ω_{SP}, ζ_{SP} aircraft short-period frequency, rad/sec, and damping ratio

Subscripts:

c command

DR Dutch roll

R roll

S spiral

ε error

A dot over a symbol indicates a derivative with respect to time.

EXPERIMENTAL PROCEDURE

A five-degree-of-freedom, fixed-base simulation study with constant airspeed was undertaken to examine the pilot's response to separation or integration of essential information in the displays. The tasks involved in these tests were to follow a prescribed path using an ILS. Two military-type three-axis gyro displays were used in the investigation. Each could display pitch, bank, and heading angles and had built-in cross-pointer needles to indicate the lateral- and vertical-displacement errors from the desired path. The displays were mounted vertically in the cockpit panel

25 cm apart. (See fig. 1.) The sensitivities of the displacement needles were held constant (for meaningful comparison) at the following values:

Vertical-displacement needle: Full deflection = 113 m

Lateral-displacement needle: Full deflection = 404 m

The sensitivities are equal to the sensitivity of an ILS at 5 n. mi. from the station. Therefore, full-scale vertical deflection would occur when the aircraft was 0.7° from the glide slope and full-scale lateral deflection would occur when the aircraft was 2.5° from the localizer. The attitude sensitivities were those defined by the size of the instrument.

Two types of tests were conducted. The first was with turbulence and the second was a step-response test without any turbulence. In the step-response tests, initial errors in both the vertical and lateral directions were included. For both types of tests, the required parameters were distributed in the two displays in several different configurations. The parameters displayed were pitch angle, bank angle, heading angle, and vertical- and lateral-displacement errors. All the subjects were given adequate practice to become familiar with the response of the system. The configuration number and the distribution of the parameters in the displays are given in the following table. The configurations were in the same sequence for all the subjects and were tested in a single sitting. The sequence was repeated again on another day.

Configuration	1	2	3	4	5	6	7	8	9
Top display	-	y	ψ	ψ,y	ϕ	ϕ,ψ	y,h	θ,h	θ,ϕ
Bottom display	y,h ϕ,ψ,θ	h ϕ,ψ,θ	y,h ϕ,θ	h θ,ϕ	y,h θ,ψ	y,h θ	θ,ϕ,ψ	y ϕ,ψ	y,h ψ

The parameters are switched from one display to the other through a switching box, thus showing a parameter at only one place during any given test. Except for controlling the desired path in both lateral and vertical modes, the subjects had no other duties to perform. Each run was conducted for about 3 min. A side-arm control stick was used as the control manipulator, and rudder pedals were not used. The control stick rotated $\pm 20^{\circ}$.

Subjects

Eight subjects participated in the tests. They ranged in experience from pilots who flew their aircraft only occasionally and who were in the process of obtaining their instrument ratings to professional test pilots. The accumulated flight hours and ages of the subjects are listed in the following table:

Initials of subject	Age	Total flight hours	IFR flight hours
MM	54	300	80
HB	44	2000	50
JS	33	3000	400
DH	23	300	50
JDS	41	300	50
JJT	37	1400	400
CP	30	1400	700
WWA	41	1600	350

Aircraft Model

A five-degree-of-freedom, nonlinear aircraft model was used in an analog computer to simulate a typical high-wing, four-place, single-engine general aviation airplane in this study. The nonlinear equations of motion used for this simulation model are presented in the appendix. The dynamic response of this simulation model to step-control inputs at the 85-knot airspeed that was used in the tests is shown in figure 2. Figure 2(a) shows the short-period longitudinal response to an elevator step input. The response is well damped and the short-period natural frequency is 2 rad/sec. The lateral dynamic response at this airspeed is shown in figure 2(b). The Dutch roll mode is fairly well damped and has a frequency of 2 rad/sec. Figure 2(b) also depicts the effect of adverse yaw on the yaw-rate response.

For further insight into the vertical and lateral responses, the linear perturbation equations of motion (obtained from the nonlinear equations given in the appendix) were written and the aircraft response characteristics were analytically determined. The linear equations of motion are the following:

$$\dot{\alpha} = \frac{F_{Z_\alpha}\alpha}{mV} + q$$

$$\dot{q} = \frac{M_{Y_\alpha}\alpha + M_{Y_q}q + M_{Y_{\delta_e}}\delta_e}{I_Y}$$

$$\dot{\beta} = \frac{F_{Y_\beta}\beta + F_{Y_p}p + F_{Y_r}r}{mV} + \frac{g}{V}\phi - r$$

$$\dot{p} = \frac{M_{X_\beta}\beta + M_{X_p}p + M_{X_r}r + M_{X_{\delta_a}}\delta_a + \left(M_{Z_\beta}\beta + M_{Z_p}p + M_{Z_r}r + M_{Z_{\delta_a}}\delta_a\right)\left(I_{XZ}/I_Z\right)}{I_X - \left(I_{XZ}^2/I_Z\right)}$$

$$\dot{r} = \frac{M_{Z_\beta}\beta + M_{Z_p}p + M_{Z_r}r + M_{Z_{\delta_a}}\delta_a + \dot{p}I_{XZ}}{I_Z}$$

At 85 knots these equations reduce to the following:

$$\dot{\alpha} = -1.03\alpha + q$$

$$\dot{q} = -1.21q - 2.82\alpha - 3.05\delta_e$$

$$\dot{\beta} = -0.229\beta - 0.994r - 0.016p + 0.225\phi$$

$$\dot{p} = -6.95\beta + 1.10r - 4.82p - 8.53\delta_a$$

$$\dot{r} = 2.85\beta - 0.725r - 0.436p + 0.216\delta_a$$

Also used for the analysis were the following linearized kinematic relationships:

$$\dot{h} = V(\theta - \alpha)$$

$$\dot{\psi} = \frac{g\phi}{V}$$

$$\dot{y} = V\psi$$

The vertical and lateral response characteristics as determined from these equations are the following:

ω_{SP} = 2.01 rad/sec $\quad \zeta_{SP}$ = 0.555 $\quad T_R$ = 0.202 sec $\quad T_S$ = 44.2 sec

ω_{DR} = 1.96 rad/sec $\quad \zeta_{DR}$ = 0.207

These analytical results agree well with the results noted from the time histories given in figure 2.

Turbulence

Two random white-noise generators were used in conjunction with two first-order filters with a time constant of 4 sec to generate the Dryden spectrum turbulence. The amplitudes of the filtered signals were adjusted to provide a 1.2 m/sec

(0.028 rad at the airspeed assumed) root-mean-square turbulence level. These random signals are added to the aerodynamic angles α and β.

Method of Analysis

A statistical analysis was performed by measuring the root-mean-square value of the deviations of the vertical and lateral paths with turbulence. A t-test was conducted to determine the level of significance of the difference in the performance obtained with each configuration and configuration 1, which was considered to be the basic reference configuration.

The pilot models were obtained by subjectively matching the step-response time histories of the pilot model-aircraft system with pilot-aircraft system simulations. Block diagrams of the pilot model-aircraft system are shown in figure 3. Decoupled and linearized diagrams are shown separated into lateral and longitudinal systems for simplicity. The pilot is represented by simple gains in the outer displacement loops (y and h) and in the heading-angle control in the middle loop for lateral motion. The inner loops θ and ϕ each contain a gain and a lag function that represent the characteristic of the response used by the pilot to place the control manipulator in the desired position. The second-order form of the response represents the associated inertia, that is, the manipulator inertia plus the pilot's muscular inertia. It also represents the critically damped response used by the pilot for the manipulator movement. The 0.2-sec lag time constant used is a preferred time constant obtained in earlier investigations. The time constant represents an undemanding control response as well as the value that the pilots use in complicated, multiloop control tasks where much of the pilot's attention must be directed to read the instruments.

A lead term can also be included in the pilot's bank-angle loop if it is required for the system stability. This lead represents the pilot's response to the rate of change of the inner-loop variable. However, in complex multiloop tasks, the pilots do not have adequate time to differentiate the inner-loop variable. In this study the lead term was assumed to be absent, even though lead time constants of 1 sec have been measured in single-loop tasks.

The relations between the aircraft control inputs δ_a and δ_e and the rate of change of inner-loop variables p and q are represented by corresponding blocks (labeled "AIRCRAFT") in the block-diagram representation of the pilot model-aircraft system shown in figure 3. The blocks represent complex relations involving many integrations, all of which are interconnected as defined by the equations of motion. In view of these complex relations, large variations in p and q due to the control surface deflections can have decided influence on the total response of the pilot-aircraft system. Investigation results of the aircraft response effects from the viewpoint of pilot models have been extensively reported in references 3 and 4.

The present study is concerned with the dynamic phase lags associated with the interrelation of the variables which the pilot is asked to regulate as subsequently described. These phase lags are shown explicitly in the block diagram of figure 3 by means of the integration terms that exist in between the variables. The 90° phase lags between ϕ and ψ and ψ and y for lateral controls and between θ and h for vertical controls dictate that coordination is required by the pilot to obtain proper system response. To control a system which contains lags such as these, it is necessary that each of these variables contribute to the control deflection. For example, in the case of lateral control the pilot model assumes that lateral

displacement is fed back to the pilot by the instrument, compared with the commanded displacement, and the resulting displacement error is used to generate a heading command. It is therefore necessary for the pilot to closely coordinate lateral displacement and heading angle. The heading-angle command is compared to the actual aircraft heading angle and the resulting heading-angle error is used to generate a bank-angle command. Therefore, heading and bank angles must be closely coordinated. The pilot's ability to provide this type of coordination is related to the ease with which he can perceive and assess the required information displayed to him. Information that can be read without much effort can be easily coordinated. This ability is the focal point of the present study.

The pilot models described in the block diagram were used to obtain time histories that could be used for comparison with actual records obtained by the test subjects. These complete-system responses were obtained using the pilot model in conjunction with the five-degree-of-freedom, nonlinear aircraft model. Both lateral and vertical pilot models were obtained from the step-response tests for each configuration. Analytically determined vertical- and lateral-system characteristics were also obtained using the linear pilot model, linear perturbation, and linearized kinematic relationships.

A representative pilot remnant was added to the output of the pilot models. This remnant was generated by passing white noise through a second-order filter identical to the pilot-model characteristic

$$\text{Remnant} = \frac{K_n}{(1 + 0.2s)^2}(\text{Random signal})$$

and adjusting the gain K_n to provide a typical remnant amplitude to match the subject's output. With this remnant, the Dutch roll mode and roll-heading mode become more visible in the time histories.

To illustrate the lateral response of the modeled pilot-aircraft system, sample time histories obtained with typical pilot-model gains and the aircraft simulation model are shown in figure 4. The associated pilot-model gains and the closed-loop system characteristics are as follows:

Pilot gains:

$K_y = 0.00183$ rad/m

$K_\psi = 0.676$

$K_\phi = 0.51$

Closed-loop system characteristics:

$\omega_y = 0.124$ $\quad \zeta_y = 0.665$

$\omega_\phi = 1.087$ $\quad \zeta_\phi = 0.924$

$\omega_{DR} = 2.123$ $\quad \zeta_{DR} = 0.179$

$\omega_C = 6.73$ $\quad \zeta_C = 0.953$

Figure 4 also illustrates the effect of remnant and limits on the bank angle and heading angle in the pilot model. The time histories in figure 4(a), which contain only linear gains in the pilot model, show a stable system. The analytically determined characteristic of the system presented in the preceding list shows a stable system. The data in the list indicate a system response which contains four modes of motion. The highest frequency control mode is derived from the pilot-model inner-loop characteristic term $(1 + 0.2s)^2$. In the complete system this mode is altered slightly by the outer-loop closures. The next lower frequency mode is the aircraft Dutch roll mode, which is also altered slightly. The next lower frequency is an oscillatory mode derived from the combination of the zero-value heading root and the lower-value roll root. The final mode of motion is derived from the zero-value lateral-displacement root and the higher value roll root. In this sample case the roots involved are a complex pair.

Figure 4(b) shows the effect of adding remnant and the limits to the pilot model. The limits added additional apparent damping to the system by limiting the excursions of ϕ and ψ, and the remnant caused lateral deviations in the steady state and made the Dutch roll oscillatory mode more visible.

It can also be seen from figure 4(b) that the bank-angle time history is dominated by the high-frequency Dutch roll mode of motion, whereas the lateral-displacement time history is dominated by the low-frequency displacement mode of motion. It is therefore necessary to scan or sample the bank-angle instrument more often than the displacement instrument in order to maintain proper control. The same situation exists for vertical control, in which the inner-loop variable (pitch angle) is dominated by the longitudinal short-period mode and therefore must be scanned more frequently than does the vertical displacement, which is dominated by a long period of motion.

RESULTS

Performance Measures

Sample time histories of the lateral and vertical deviations from the desired path for runs with turbulence are shown in figures 5 to 7. The histories shown are for subjects CP, JS, and DH, and the display configurations used were 1, 5, 6, and 7. It can be seen from these figures that there are apparent differences in lateral-mode response, whereas the vertical mode does not change much except for configuration 7, for which a small reduction in error can be seen.

Root-mean-square values of the lateral and vertical deviations for all the subjects are given in table 1, together with averages of the scores and their standard deviations. In addition, t-tests were performed to determine any significant difference between the reference configuration (configuration 1, which has all the parameters displayed together) and the rest of the configurations. The results of the t-tests are shown in table 2. A P-value of 0.025 is considered to be significant. The t-tests show that there are significant differences in the lateral-mode scores with respect to configuration 1 for configurations 2, 5, and 7. The rms table shows that configuration 5 is worse than configuration 1, whereas configurations 2 and 7 are better than configuration 1. For configuration 5, the bank angle alone is displayed separately from the rest of the parameters, whereas for configuration 7 both vertical and lateral displacements are presented together in one display with the rest of the parameters in another display. The t-tests performed for the vertical mode show no significant differences between the configurations, although

configuration 7 does seem to show better performance, with a P-value of 0.04 when compared with configuration 1. The average value of the scores for all the subjects for vertical control does seem to be greater in configurations 5, 6, and 8 when compared with configuration 1. (See table 1.)

Because configuration 7 gave the best performance, separate experiments were conducted with the same parameter-display arrangement (i.e., all attitudes displayed together and separate from the displacement data) as configuration 10. For configuration 10, however, the displacement errors were displayed on glide-slope needle (for Δh) and turn-indicator needle (for y) in the same instrument (fig. 1) instead of cross-pointer needles in the second instrument. All eight subjects again participated in the experiments. Configuration 1 was again repeated in conjunction with making these additional tests on configuration 10. The scores obtained with these tests are tabulated and are presented in table 3.

The results of these experiments indicate that the repeated performance for configuration 1 does not significantly differ from that of the earlier experiments. Configuration 10 is significantly better than the repeated configuration 1 and does not significantly differ from configuration 7. Thus, separating the displacements and combining all the attitudes does indeed give the best performance.

System Analysis

To gain further insight into the differences between the configurations, a pilot model-aircraft system analysis was performed for step-input tests. The closed-loop system characteristics for the lateral mode for all the subjects using various configurations are shown in table 4, and the disposition of the roots in s-plane for configurations of interest are shown in table 5. Typical response time histories for step-input tests for subjects WWA, MM, and CP are shown in figures 8 to 10 along with the responses obtained with the corresponding models. The tests indicate that the subjects had maximum gains for configurations 1 and 7, as shown in table 6, and produced stable responses for these configurations. The gains K_ϕ and K_y are reduced for configuration 5 with no appreciable change in K_ψ. The gains in configuration 6 are restored almost to those of configuration 1. Also, the tests indicate that configuration 5 produces either a sluggish response or reduced damping leading into instability when compared with a good stable response with configuration 1. Time histories of the subjects shown in figures 8 to 10 illustrate this point.

The lowest frequency root (y mode), which is a complex root for configuration 1 in all cases except one, becomes a pair of separated real roots for configuration 5. The next higher frequency root (roll-heading angle mode) always becomes a complex pair. Representative movement of the closed-loop poles for subjects MM, DH, and CP is shown in figure 11. The figure illustrates that the subject MM moved one of the real roots for configuration 5 nearer to the imaginary axis, thus making the response due to this root sluggish while producing considerable reduction in damping and frequency in the roll-heading angle mode, leading to instability. Although the y-mode roots are well placed in the cases of subjects CP and DH, nevertheless they produced highly reduced frequencies in the roll-heading angle mode root, thus making the system sluggish in response due to this root. The system response, which became poor with configuration 5, improved considerably with configuration 6, for which heading and bank angles are displayed together, and it becomes even better with configuration 7.

DISCUSSION

From the preceding results, it can be seen that separating the bank-angle information from heading-angle information seems to cause a marked deterioration in the pilot-aircraft system performance in lateral control, which may at times prove to be detrimental to accomplishing the mission. This fact is evident from both turbulence and step-response tests. The reason for this deterioration can be explained in terms of the pilot model-aircraft system. The high-frequency bank angle, which forms the innermost loop in lateral control, must be monitored by the pilot at a higher rate and should be closely coordinated with heading angle for proper lateral position control. The displacement information, forming the lowest frequency outermost loop, is scanned at a relatively lower rate than the bank angle and heading angle. Hence, the displacement information, although it must be coordinated with heading angle, can be separated from heading and bank angles without any deterioration in the system performance, as the results for configurations 2 and 7 show. For configuration 6, with bank angle and heading angle also displayed together, the pilot is able to achieve a pilot-aircraft system performance which is almost on the level of configuration 1.

Configuration 3 is a case for which heading and bank angles are separated but bank angle is displayed together with pitch angle, which forms the inner loop for the vertical control. This situation produced only slightly improved control when compared with configuration 5, with certain characteristic differences from configuration 6. Configuration 6 produced relatively more damping in the roll-heading angle mode than configuration 3 in a majority of the cases. This tendency is also confirmed from results for configuration 4 and separate tests with bank angle and pitch angle displayed together (configuration 9), which were performed with only three subjects. The reason for the slight improvement over configuration 5 in system performance for configuration 3 could be that when the pilot has to control both lateral and vertical modes simultaneously, displaying the most frequently scanned inner-loop parameters θ and ϕ together helps him to obtain better coordination. When heading angle is also displayed together with pitch and bank attitudes, there is further improvement with very good overall system performance, as seen for configuration 7. For configuration 7, separating the displacements produces less clutter in the displays and gives better performance than the other configurations. Configuration 8 shows some mixed results and the subjects observed that it is an unconventional display configuration as it completely isolates lateral and vertical modes.

In the case of vertical control, no appreciable changes occur in the pilot gains K_θ and K_h for all configurations for which pitch and bank angles are displayed together, whereas K_θ appears to be slightly lower for configurations for which θ and ϕ are separated. An output record of subject HB and corresponding pilot-model output for configuration 1 are shown in figure 12. The respective gains and the associated closed-loop parameters for vertical control are as follows:

Pilot gains:

$K_h = 0.0014$ rad/m $\qquad K_\theta = 0.183$

Closed-loop system characteristics:

$\omega_h = 0.093$ $\quad \zeta_h = 0.72$

$\omega_\alpha = 1.870$ $\quad \zeta_\alpha = 0.86$

$\omega_C = 5.320$ $\quad \zeta_C = 0.98$

It is observed from the records of the simulator runs and the model matching that with the aircraft dynamics of the type simulated and with the type of display instruments used, all the subjects showed certain limits in heading-angle, bank-angle, and pitch-angle changes used for accomplishing the step-displacement corrections. The values of these limits tended to change with configuration of the displays, as shown in table 7. These limit values were obtained from the model matching. The average of the heading-angle limit for configuration 1 is 0.17 rad (10°). For this configuration all the subjects showed a limit on the heading angle. As for the bank angle, the majority of the subjects observed limits on both initial bank-angle change that is used for obtaining the required heading angle as well as the subsequent bank-angle change in the other direction used to bring the heading angle to zero.

For configuration 5, the limits to which the subjects allowed the attitudes to change for accomplishing the task fall under two categories. The subjects either did not allow as much heading-angle and bank-angle changes as they allowed in configuration 1, or they showed no apparent limits to the changes. In the first case the subjects used attitudes much smaller than those for configuration 1, and in the second case the maximum values were very much larger than those used for configuration 1. The lower limits contributed to sluggish responses whereas the "no limits" are associated with reduced damping and instability. It can also be seen that for configurations 2, 3, 4, 6, and 7 the subjects used approximately the same limits as they used for configuration 1.

With favorable dynamics and display configuration, if the pilots achieve stable responses with higher limit values, it reflects a better control situation with that configuration than with either the unstable control with higher limits or the sluggish response with lower limits.

The model-matching analysis shows that the linear model, with the addition of saturation limits and the addition of remnant, reproduces most of the characteristics of pilot-generated time histories. The frequencies and damping of the different modes of motion that are most prominent in the time histories are reproduced by the composite pilot model. However, sample time histories also show that there are certain characteristics of the pilot-generated response that are not reproduced by the pilot model. The unmatched characteristics are slow divergences that occur near the end of some of the runs that probably result from a lack of attention on the part of the pilot, and a discretized, on-off type of response that can be detected in some of the records that probably results from a dead band or indifference level on the part of the subject. It is believed that even though the model used on this analysis does not match all of the characteristics of the subject pilots, it nevertheless does provide a very useful insight into the pilot response.

CONCLUDING REMARKS

A fixed-base simulation study was conducted using military three-axis gyro displays (with cross-pointer needles for displacement information) to ascertain the

effects on manual aircraft control of parameter separation in displays. The effects in terms of pilot models and pilot-aircraft system closed-loop performance were obtained. A typical general aviation airplane dynamic model was used in the study. Eight subjects with various amounts of experience participated in the study. The aircraft was assumed to be at a position 5 n. mi. from the instrument landing system (ILS) station in the landing-approach condition. Attitudes (including the heading angle) and displacement errors from localizer and glide slope were displayed to the pilot.

Bank angle, heading angle, and pitch angle together in one instrument with the displacements displayed in another location produced the best performance in both lateral and vertical controls by the pilot. Statistical analysis of the path-following task with turbulence showed that the accuracy of the path following was good when all the parameters were displayed together in one location (reference configuration) and proved to be still better when the displacements together were displayed in one location and the attitudes together are displayed in another location. Accuracy of the lateral path following became poor and significantly different from the reference configuration for the configuration with bank angle displayed separately from the rest of the parameters. The lateral performance improved considerably in the path-following task when the bank angle and heading angle were displayed together. No significant differences were observed in the vertical-control mode.

Time-history plots and the pilot model-aircraft system analysis indicate that the system was stable in the reference configuration in both axes. The pilots reduced their gains in the bank angle and displacement loops when the bank angle was displayed separately, causing the system to become either sluggish or poorly damped, causing instability in the lateral control. It was also observed that a combination of bank angle and heading angle produced a system which had better damping in lateral control than a configuration for which pitch and bank angles were combined and separated from the heading. The display location of the displacements did not affect the performance as much as separating the displacements from the attitudes, which seemed to reduce the clutter of information and provided better control in both modes.

It was also observed that the subjects imposed limits on changes in the heading angle, bank angle, and pitch angle to accomplish the desired task under step-input tests. The limit values were maximum when all the parameters were displayed together (reference configuration). There were either "no limits" or considerably reduced limits when the bank angle was displayed separately, thus producing either a poorly damped system or sluggish response.

Langley Research Center
National Aeronautics and Space Administration
Hampton, VA 23665
August 12, 1981

APPENDIX

AIRCRAFT EQUATIONS OF MOTION

The equations of motion for the aircraft simulation used in the study are the following:

$$\dot{\alpha} = -1.03\alpha + q - 0.225(1 - \cos\theta \cos\phi)$$

$$\dot{q} = -1.21q - 2.82\alpha - 3.05\delta_e$$

$$\dot{p} = -4.82p + 1.10r - 6.95\beta - 8.53\delta_a$$

$$\dot{r} = -0.436p - 0.725r + 2.85\beta + 0.216\delta_a$$

$$\dot{\beta} = -0.016p - 0.994r - 0.229\beta + 0.225(\sin\phi \cos\theta)$$

$$\dot{\phi} = p + \dot{\psi} \sin\theta$$

$$\dot{\theta} = q \cos\phi - r \sin\phi$$

$$\dot{\psi} = \frac{r \cos\phi + q \sin\phi}{\cos\theta}$$

$$\dot{h} = V(\theta - \alpha)$$

$$\dot{y} = V\psi$$

REFERENCES

1. Adams, James J.: Simulator Study of Conventional General Aviation Instrument Displays in Path-Following Tasks With Emphasis on Pilot-Induced Oscillations. NASA TP-1776, 1980.

2. Levison, William H.; and Elkind, Jerome I.: Two-Dimensional Manual Control Systems With Separate Displays. Third Annual NASA-University Conference on Manual Control, NASA SP-144, 1967, pp. 29-42.

3. Adams, James J.; and Hatch, Howard G., Jr.: An Approach to the Determination of Aircraft Handling Qualities by Using Pilot Transfer Functions. NASA TN D-6104, 1971.

4. Adams, James J.; and Moore, Frederick L.: An Analytical Study of Aircraft Lateral-Directional Handling Qualities Using Pilot Models. NASA TN D-8103, 1976.

TABLE 1.- SCORES, AVERAGES, AND STANDARD DEVIATIONS

[All values are in meters]

Subject	Day	Root-mean-square lateral and vertical deviations for configuration[a] -																	
		1		2		3		4		5		6		7		8		9	
		Δh	y	Δh	y	Δh	y	Δh	y	Δh	y	Δh	y	Δh	y	Δh	y	Δh	y
MM	1	9.1	32.2	9.1	16.2	9.1	24.3	6.8	48.7	9.1	24.3	6.8	24.3	2.3	24.3	2.3	40.1	6.9	
	2	9.1	24.3	4.5	24.3	6.8	40.6	6.8	40.6	6.8	24.3	6.8	40.6	6.8	24.3	11.3	24.3		
HB	1	4.5	16.2	4.5	24.3	4.5	16.2	4.5	16.2	2.3	24.3	4.5	16.2	6.8	16.2	6.8	24.3		
	2	6.8	8.1	6.8	24.3	4.5	40.6	9.1	32.4	4.5	16.2	6.8	32.4	5.5	16.2	2.3	16.2		
JS	1	6.8	32.4	2.3	24.3	5.7	24.3	4.5	32.4	6.8	32.2	6.8	32.4	2.3	12.2	9.1	32.4	4.5	32.4
	2	5.7	24.3	4.5	8.1	6.8	24.3	2.3	24.3	9.1	48.7	11.3	32.4	2.3	16.2	6.8	32.4		
DH	1	9.1	40.6	6.8	24.3	6.8	32.2	4.5	40.6	11.3	48.7	6.8	40.6	9.1	16.2	6.8	48.7		
	2	6.8	32.2	4.5	24.3	6.8	24.3	13.6	32.4	11.3	48.7	13.6	40.6	2.3	32.4	9.1	32.4		
JDS	1	6.8	48.7	6.8	16.2	6.8	48.7	11.3	64.9	18.1	73.0	11.3	40.6	6.78	32.4	11.3	81.1		
	2	11.3	32.2	6.8	8.1	7.91	40.6	5.7	32.4	7.9	48.7	13.6	40.6		24.3	4.5	32.4		
JJT	1	6.8	32.2	9.1	24.3	7.9	32.2	4.5	32.4	9.1	32.2	9.1	40.6	5.65	24.3	5.7	32.4		
	2	6.8	32.2	5.7	24.3	5.65	32.2	4.5	40.6	5.7	24.3	6.8	24.3						
CP	1	6.8	24.3	3.4	24.3	6.8	32.2	4.5	16.2	9.1	64.8	11.3	32.2	5.5	16.2	11.3	40.6	5.6	24.8
	2	5.7	32.2	6.8	24.3	9.1	32.2	6.8	36.5	11.3	32.2	17.0	20.3	9.1	32.4	15.8	32.4		
WWA	1	9.1	56.8	11.3	48.6	9.1	48.7	6.8	32.4	11.3	73.0	7.9	40.6	5.7	24.3	4.5	40.6		
	2	4.5	48.7	9.1	40.6	11.3	40.6	6.8	32.4	6.8	81.1	5.6	20.3	7.9	32.4	9.1	60.8		
Average		7.2	32.2	6.6	23.9	7.2	33.7	6.4	34.9	8.8	43.8	9.2	33.2	5.4	23.1	8.0	38.1		
Standard deviation		1.8	12.2	2.3	10.5	1.8	9.3	2.82	11.8	3.6	17.6	3.5	8.1	2.5	7.3	3.7	15.8		

[a]The configurations used were as follows:

Configuration	1	2	3	4	5	6	7	8	9
Top display		y	ψ	ψ,y	ϕ	ϕ,ψ	y,h	θ,h	θ,ϕ
Bottom display	y,h ϕ,ψ,θ	h ϕ,ψ,θ	y,h ϕ,θ	h ϕ,θ	y,h ψ,θ	y,h θ	ϕ,ψ,θ	y ϕ,ψ	y,h ψ

TABLE 2.- RESULTS OF t-TESTS ON SCORES FOR CONFIGURATION 1

AND THE OTHER CONFIGURATIONS

Parameter	Probability for configurations -						
	1 and 2	1 and 3	1 and 4	1 and 5	1 and 6	1 and 7	1 and 8
h	0.15	0.5	0.18	0.06	0.03	0.04	0.34
y	0.010	0.360	0.240	0.003	0.400	0.001	0.030

TABLE 3.- SCORES, AVERAGES, AND STANDARD DEVIATIONS OF

CONFIGURATION 1 (REPEATED) AND CONFIGURATION 10

[All values are in meters]

Subject	Day	Root-mean-square lateral and vertical deviations for configuration -			
		1 (repeated)		10	
		Δh	y	Δh	y
MM	1	8.8	40	6.6	16
	2	8.8	28	6.6	18
HB	1	4.4	28	4.4	16
	2	4.4	40	4.4	16
JS	1	4.4	16	2.2	16
	2	2.2	28	2.2	20
DH	1			4.4	24
	2			6.6	16
JDS	1	11.0	40	11.0	32
	2	15.0	40	8.8	40
JJT	1	8.8	40	13.2	25
	2	6.6	48	6.0	
CP	1	4.0	16	2.2	10
	2	4.4	16	4.4	32
WWA	1	11.0	56	8.8	40
	2	6.6	40	6.6	24
Average		7.2	33	6.2	24
Standard deviation		3.6	12.1	3.1	9.8

TABLE 4.- PILOT MODEL-AIRCRAFT SYSTEM CHARACTERISTICS FOR LATERAL MODE

Subject	Root	Closed-loop system characteristics for configuration - 1		2		3		4		5		6		7		8		9	
		ω, rad/sec	ζ	ω, rad/sec	ζ	ω, rad/sec	ζ	ω, rad/sec	ζ	ω, rad/sec	ζ	ω, rad/sec	ζ	ω, rad/sec	ζ	ω, rad/sec	ζ	ω, rad/sec	ζ
MM	γ_y	0.187	0.864	0.167	0.946	0.204	0.800	[a]-0.305	[a]-0.070	[a]-2.815	[a]-0.079	[a]-0.222	[a]-0.040	[a]-0.242	[a]-0.100	[a]-0.224	[a]-0.210	0.208	0.866
	γ_ϕ	1.333	.493	1.170	.672	1.405	.428	1.600	.304	.251	.298	1.216	.651	1.155	.673	1.098	.678	1.343	.469
	γ_{DR}	2.380	.104	2.224	.150	2.504	.068	3.477	-.157	2.001	.197	2.238	.151	2.223	.149	2.217	.146	2.413	.092
	γ_C	7.260	.938	6.983	.946	7.444	.933	8.556	.906	6.145	.971	7.006	.945	6.980	.946	6.974	.946	7.315	.936
HB	γ_y	0.205	0.907	[a]-0.301	[a]-0.105	[a]-0.444	[a]-0.076	0.186	0.972	0.180	0.959	[a]-0.215	[a]-0.064	[a]-0.271	[a]-0.116	0.144	0.892		
	γ_ϕ	1.316	.488	1.231	.554	1.234	.500	1.248	.557	1.342	.476	1.137	.743	1.063	.757	1.148	.744		
	γ_{DR}	2.381	.100	2.300	.128	2.332	.106	2.304	.125	2.404	.097	2.189	.161	2.185	.158	2.189	.162		
	γ_C	7.266	.938	7.130	.942	7.192	.939	7.137	.941	7.300	.937	6.904	.948	6.897	.948	6.905	.948		
JS	γ_y	[a]-1.541	[a]-0.103	[a]-0.442	[a]-0.138	[a]-0.720	[a]-0.125			[a]-0.280	[a]-0.121	0.195	0.582	[a]-0.816	[a]-0.088	[a]-1.553	[a]-0.099		
	γ_ϕ	.566	.560	1.182	.519	.934	.610			1.125	.669	1.186	.715	.801	.726	.568	.554		
	γ_{DR}	2.109	.168	2.303	.111	2.208	.137			2.222	.148	2.204	.158	2.169	.154	2.108	.168		
	γ_C	6.701	.954	7.148	.941	6.964	.946			6.983	.946	6.939	.947	6.867	.949	6.698	.954		
DH	γ_y	0.139	0.828	[a]-0.194	[a]-0.078					[a]-2.016	[a]-0.378	0.154	0.749	0.180	0.875	0.144	0.832	0.144	0.832
	γ_ϕ	1.368	.495	1.412	.439					.086	.898	1.368	.496	1.336	.492	1.263	.610	1.262	.610
	γ_{DR}	2.396	.110	2.493	.079					2.052	.192	2.396	.110	2.386	.104	2.269	.143	2.512	.129
	γ_C	7.278	.938	7.421	.934					6.464	.961	7.278	.938	7.270	.938	7.067	.943	7.04	.947
JDS	γ_y	0.216	0.932	[a]-0.255	[a]-0.049	[a]-0.302	[a]-0.019	0.179	0.691	0.148	0.870	0.166	0.765	[a]-0.469	[a]-0.110	[a]-2.027	[a]-0.074		
	γ_ϕ	1.195	.589	1.007	.911	1.340	.487	1.408	.450	1.358	.494	1.358	.498	1.038	.656	.521	.389		
	γ_{DR}	2.272	.131	2.135	.178	2.390	.105	2.477	.085	2.393	.108	2.393	.108	2.217	.142	2.065	.177		
	γ_C	7.084	.943	6.766	.952	7.271	.938	7.399	.934	7.276	.936	7.276	.938	6.977	.946	6.536	.958		
JJT	γ_y	0.230	0.905	[a]-0.235	[a]-0.0917	[a]-0.159	0.918	0.209	0.901	[a]-0.290	[a]-0.048	0.275	0.073	[a]-0.210	[a]-0.132	0.260	0.591	0.235	0.956
	γ_ϕ	1.244	.535	1.409	.426	1.484	.377	1.376	.436	1.307	.511	1.302	.511	1.303	.513	1.307	.529	1.246	.518
	γ_{DR}	2.318	.116	2.509	.068	2.693	.020	2.470	.073	2.355	.113	2.353	.122	2.353	.112	2.350	.113	2.329	.110
	γ_C	7.168	.940	7.448	.933	7.684	.927	7.400	.934	7.218	.939	7.218	.939	7.218	.939	7.218	.939	7.188	.940
CP	γ_y	0.237	0.941	[a]-0.415	[a]-0.0758	0.190	0.918			[a]-1.282	[a]-0.226	0.268	0.847	0.212	0.670	[a]-0.295	[a]-0.027		
	γ_ϕ	1.095	.673	1.084	.660	1.247	.564			.586	.577	1.200	.557	1.277	.567	1.269	.556		
	γ_{DR}	2.219	.144	2.221	.144	2.298	.128			2.133	.160	2.293	.120	2.304	.129	2.307	.128		
	γ_C	6.981	.946	6.980	.946	7.128	.942			6.780	.951	7.127	.941	7.137	.941	7.136	.941		
WWA	γ_y	0.089	0.761	0.124	0.665			0.286	0.874	[a]-1.417	[a]-0.492	[a]-0.233	[a]-0.090	0.168	0.932	[a]0.212	[a]0.102		
	γ_ϕ	1.406	.496	1.087	.924			1.055	.683	.233	.789	1.165	.673	1.169	.675	1.236	.595		
	γ_{DR}	2.409	.117	2.123	.179			2.210	.143	2.103	.178	2.22	.150	2.223	.151	2.275	.137		
	γ_C	7.288	.937	6.730	.953			6.970	.946	6.670	.955	6.98	.946	6.980	.946	7.081	.943		

[a]Real root.

TABLE 5.- DISPOSITION OF FIRST TWO CLOSED-LOOP ROOTS

OF PILOT-AIRCRAFT SYSTEM IN COMPLEX PLANE

Subject	Root	Disposition of closed-loop roots for configuration - 1		5		6		7	
		$\zeta\omega_n$	ω_d	$\zeta\omega_n$	ω_d	$\zeta\omega_n$	ω_d	$\zeta\omega_n$	ω_d
MM	γ_y	0.161	0.094	[a]-0.079	[a]-2.815	[a]-0.040	[a]-0.222	[a]-0.100	[a]-0.242
	γ_ϕ	.657	1.159	.075	.239	.791	.923	.777	.854
HB	γ_y	0.185	0.086	0.172	0.050	[a]-0.064	[a]-0.271	[a]-0.116	[a]-0.271
	γ_ϕ	.642	1.149	.638	1.180	.844	.760	.804	[a]1.047
JS	γ_y	[a]-0.103	[a]-1.541	[a]-0.121	[a]-0.280	0.113	0.158	[a]-0.088	[a]-0.816
	γ_ϕ	.317	.469	.752	.836	.848	.829	.585	.550
DH	γ_y	0.115	0.078	[a]-0.378	[a]-2.016	0.115	0.102	0.157	0.080
	γ_ϕ	.677	1.188	.077	.037	.678	1.187	.657	1.163
JDS	γ_y	0.201	0.216	0.128	0.086	0.126	0.107	[a]-0.110	[a]-0.469
	γ_ϕ	.703	.965	.670	1.181	.676	1.177	.680	.783
JJT	γ_y	0.208	0.098	[a]-0.048	[a]-0.290	[a]-0.110	[a]-0.469	[a]-0.110	[a]-0.469
	γ_ϕ	.666	1.051	.667	1.230	.665	1.23	.668	1.230
CP	γ_y	0.223	0.080	[a]-0.226	[a]-1.282	0.226	0.142	0.142	0.157
	γ_ϕ	.737	.810	.338	.478	.668	.996	.724	1.052
WWA	γ_y	0.067	0.058	[a]-0.492	[a]-1.417	[a]-0.090	[a]-0.233	0.156	0.061
	γ_ϕ	.697	1.221	.183	.143	.784	.862	.789	.863

[a]Real root.

TABLE 6.- PILOT GAINS FOR SELECTED CONFIGURATIONS

Subject	Pilot gains for configuration -											
	1			5			6			7		
	K_y, μrad/m	K_ψ	K_ϕ	K_y, μrad/m	K_ψ	K_ϕ	K_y, μrad/m	K_ψ	K_ϕ	K_y, μrad/m	K_ψ	K_ϕ
MM	0.00229	1.25	-1.10	0.00148	1.41	-0.17	0.00078	0.95	-0.78	0.00149	1.17	-0.75
HB	.00238	1.40	-1.10	.00106	.97	-.67	.00167	.97	-.67	.00166	1.23	-.67
JS	.00185	1.83	-.51	.00176	1.32	-.76	.00316	.96	-.71	.00158	1.67	-.66
DH	.00182	.94	-1.10	.00096	.56	-.32	.00219	.95	-1.10	.00219	1.23	-1.10
JDS	.00238	1.42	-1.28	.00184	1.04	-1.10	.00231	1.04	-1.10	.00184	1.62	-.76
JJT	.00262	1.50	-.98	.00092	1.24	-1.04	.00127	1.28	-1.04	.00175	1.28	-1.04
CP	.00249	1.46	-.76	.00316	1.94	-.60	.00315	1.60	-.94	.00316	1.15	-.93
WWA	.00129	.58	-1.10	.00238	1.13	-.47	.00138	1.13	-.75	.00186	1.12	-.75

TABLE 7.- LIMIT VALUES OF YAW AND ROLL ANGLES FOR VARIOUS CONFIGURATIONS

[Values are in radians]

Subject	Limit values for configuration -																	
	1		2		3		4		5		6		7		8		9	
	ψ	ϕ	ψ	ϕ	ψ	ϕ	ψ	ϕ	ψ	ϕ	ψ	ϕ	ψ	ϕ	ψ	ϕ	ψ	ϕ
HB	0.16	+0.09 -.11	0.12	+0.09 -.07	0.16	+0.09 -.07	0.15	+0.08 -.09	0.09	+0.10 -.09	0.13	+0.07 -.07	0.13	+0.09 -.07	0.11	+0.08 -.07		
JS	0.28	+0.35 -.43		+0.25 -.35		+0.25 -.35		+0.25 -.35				+0.28		+0.28 -.23		+0.28 -.24		
DH	0.18	-0.08	0.16	+0.08 -.08	0.12	+0.06 -.06	0.09	+0.06 -.06			0.11	+0.06 -.07	0.14	+0.11 -.07	0.11	+0.10 -.11	0.11	+0.10 -.10
JDS	0.14	+0.08 -.07	0.18	+0.10 -.06	0.23	+0.14	0.17	+0.12 -.09	0.16	+0.04 -.08	0.16	+0.10 -.08	0.16	+0.09 -.10	0.13	+0.08 -.09		
CP	0.17	+0.11	0.16	+0.11 -.07	0.19	+0.16 -.12	0.12	+0.12 -.08		+0.04 -.20	0.14	+0.09 -.19	0.09	+0.06	0.07	+0.06 -.04		
JJT	0.10	+0.12 -.08	0.12	+0.06 -.07	0.11	+0.06 -.06	0.10	+0.06 -.05	0.07	+0.08 -.04	0.11	+0.08 -.06	0.08	+0.08 -.06	0.09	+0.11 -.07	0.11	+0.07 -.09
WWA	0.17	+0.12 -.08	0.18	+0.12 -.10	0.18	+0.11 -.09	0.16	+0.12	0.16	+0.12	0.14	+0.08 -.06	0.14	+0.07 -.05	0.14	+0.07 -.06		

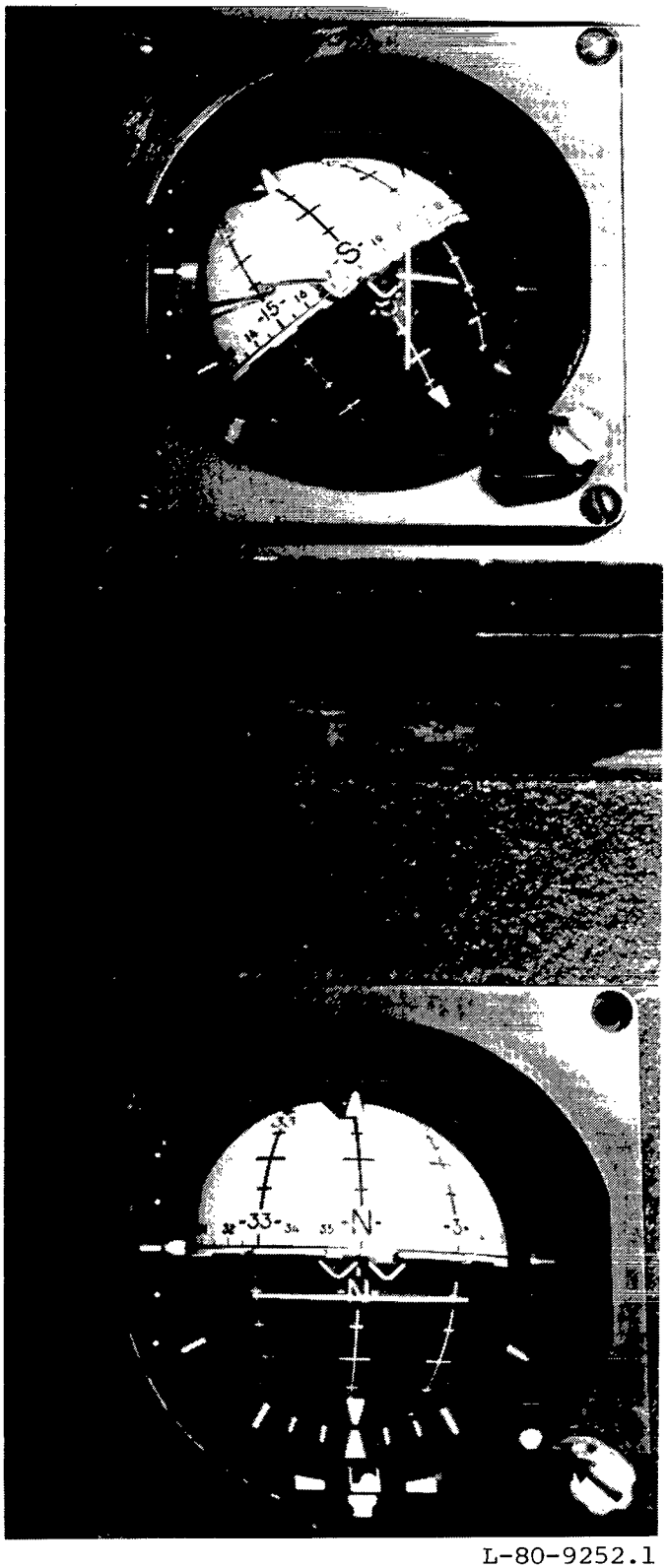

L-80-9252.1

Figure 1.- Instrument display.

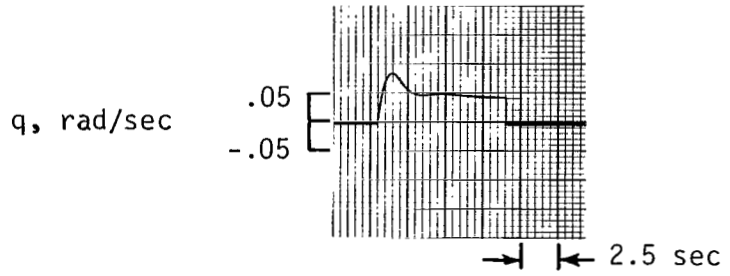

(a) Short-period longitudinal response to a 0.069 rad elevator step.

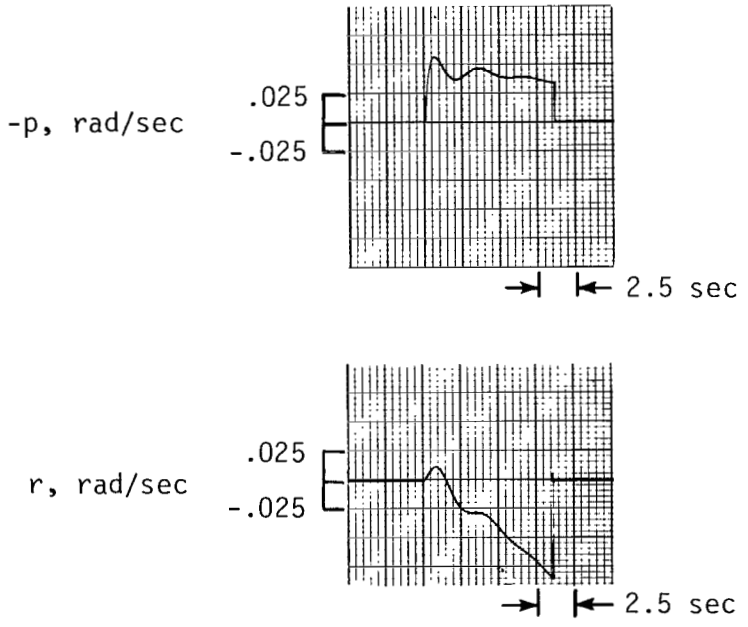

(b) Lateral dynamic response and yaw-rate response to a 0.035 rad aileron step.

Figure 2.- Step-control-input responses.

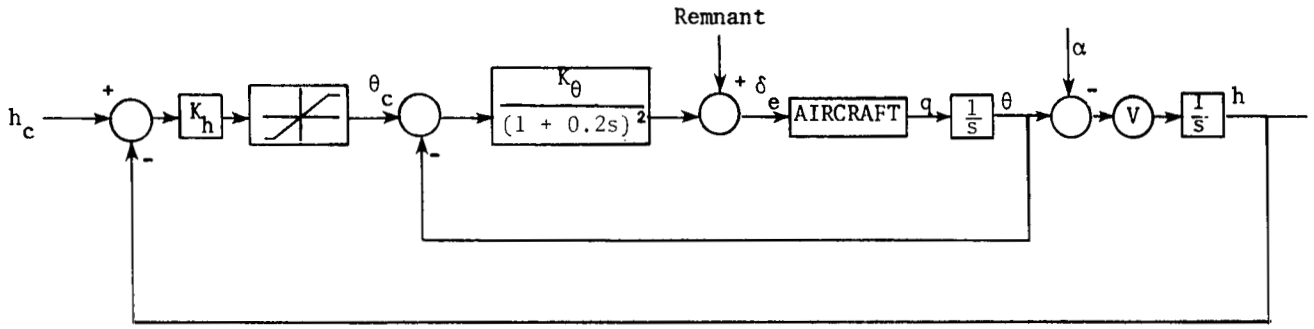

(a) Longitudinal system.

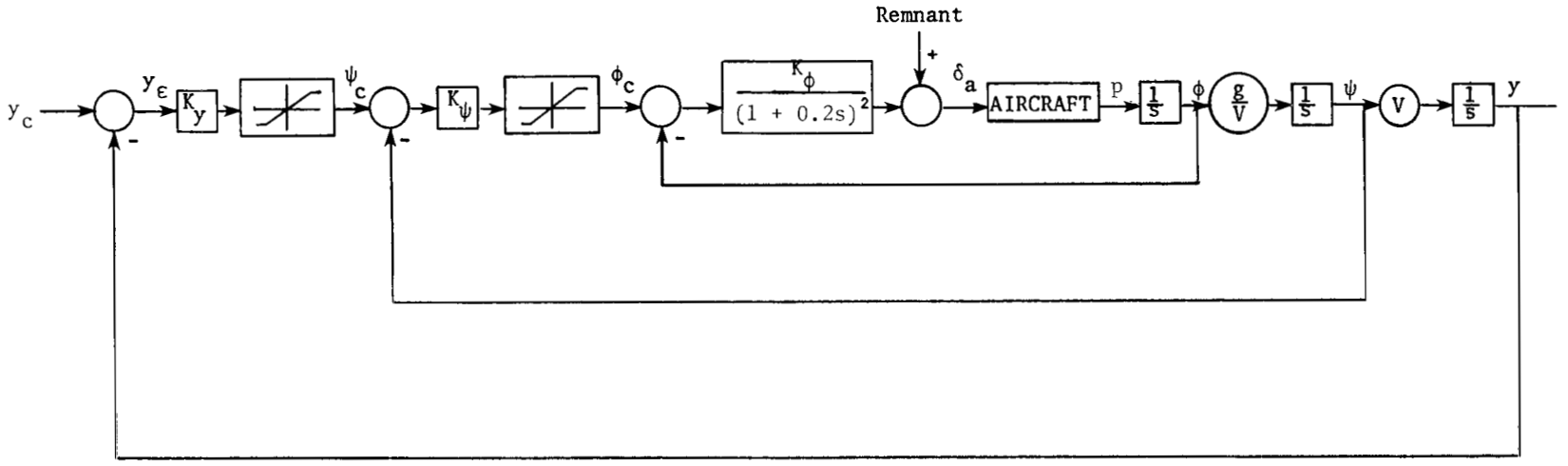

(b) Lateral system.

Figure 3.- Pilot model-aircraft system.

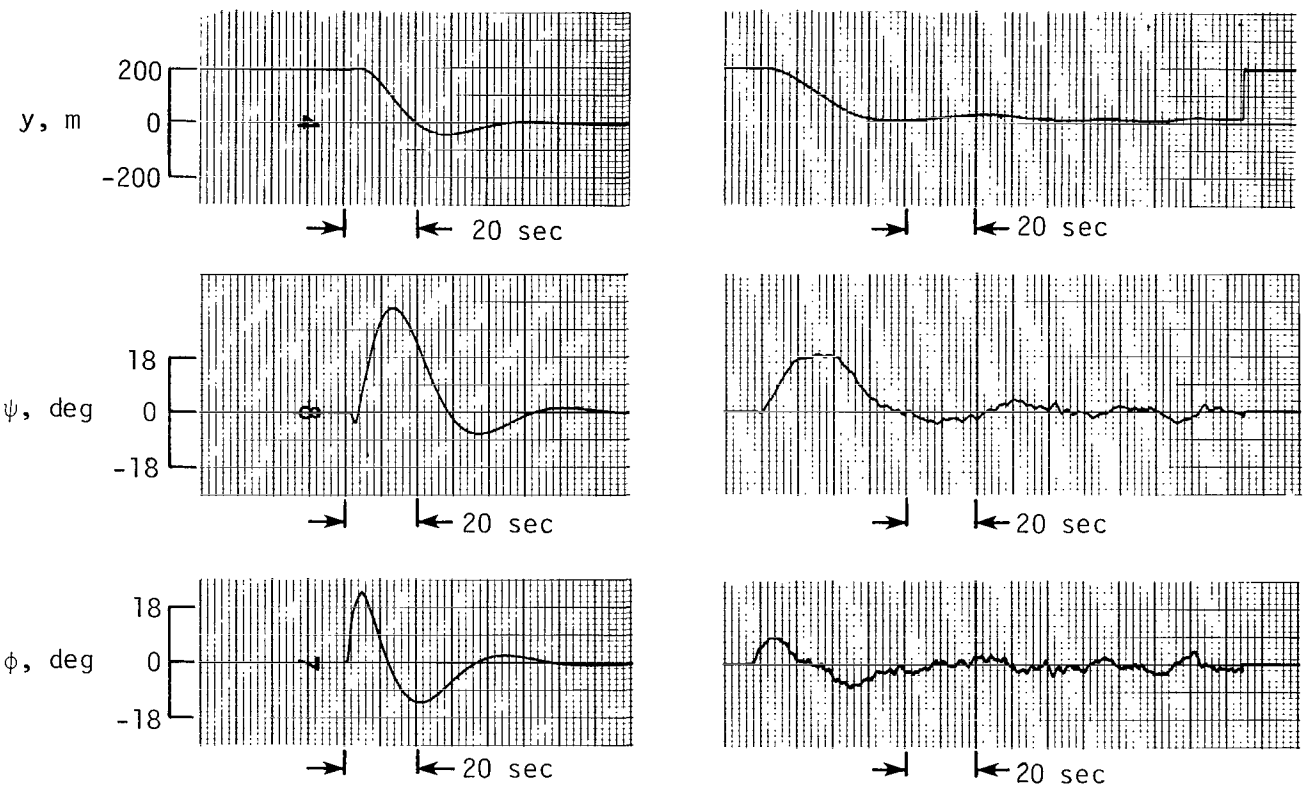

(a) Linear system only.

(b) Complete system with limits and remnant.

Figure 4.- Pilot model-aircraft system lateral response. $K_{\phi} = -0.51$; $K_{\psi} = 0.676$; $K_{y} = 0.00183$ rad/m.

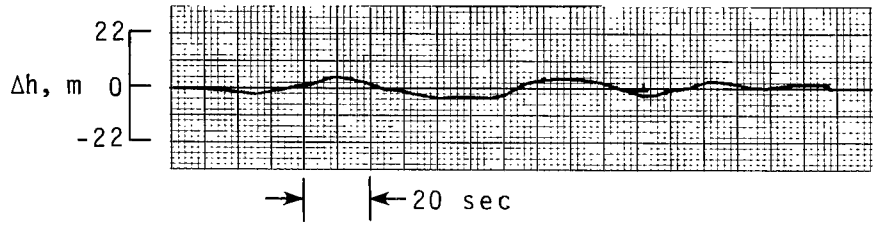

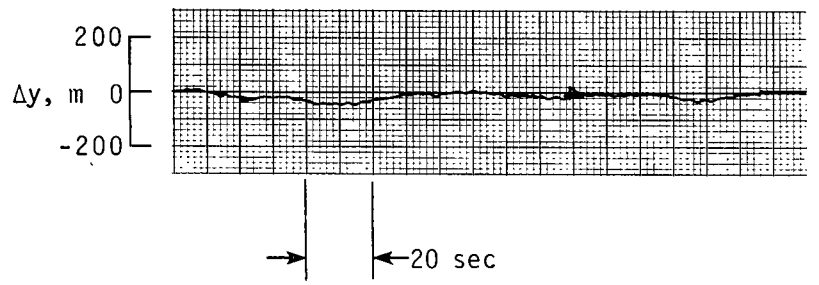

(a) Configuration 1.

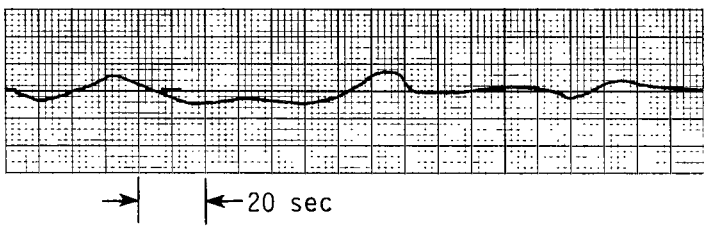

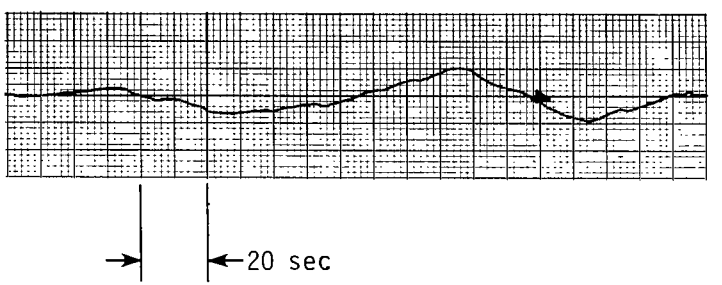

(b) Configuration 5.

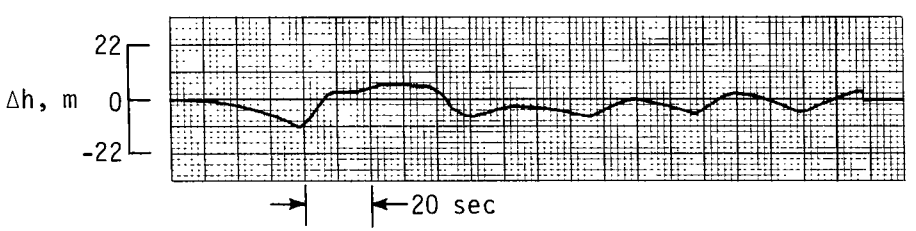

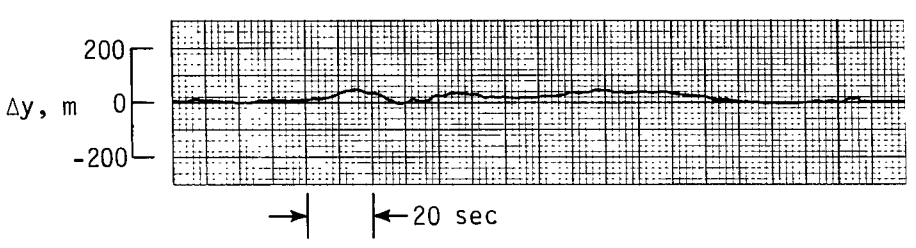

(c) Configuration 6.

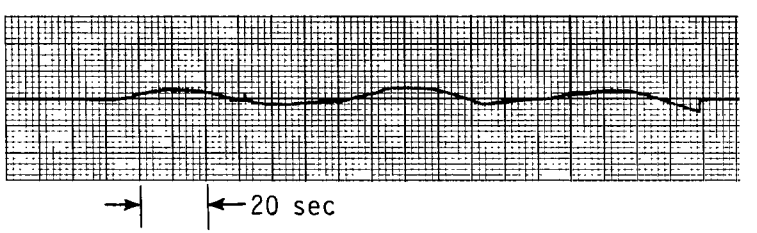

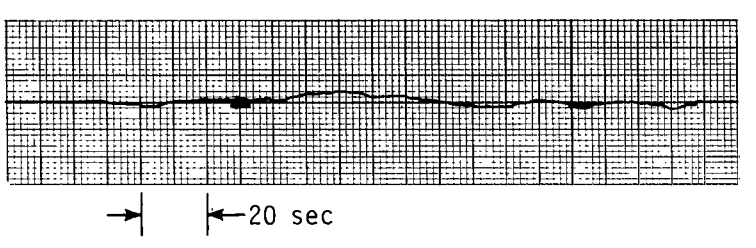

(d) Configuration 7.

Figure 5.- Sample time histories with turbulence for subject CP.

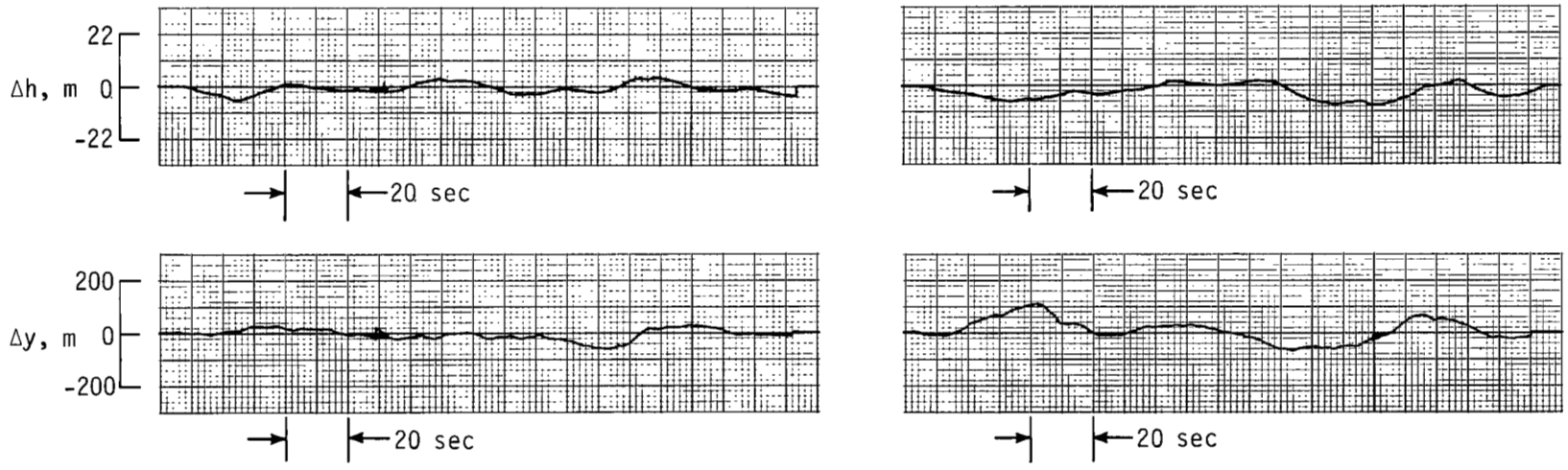

(a) Configuration 1.

(b) Configuration 5.

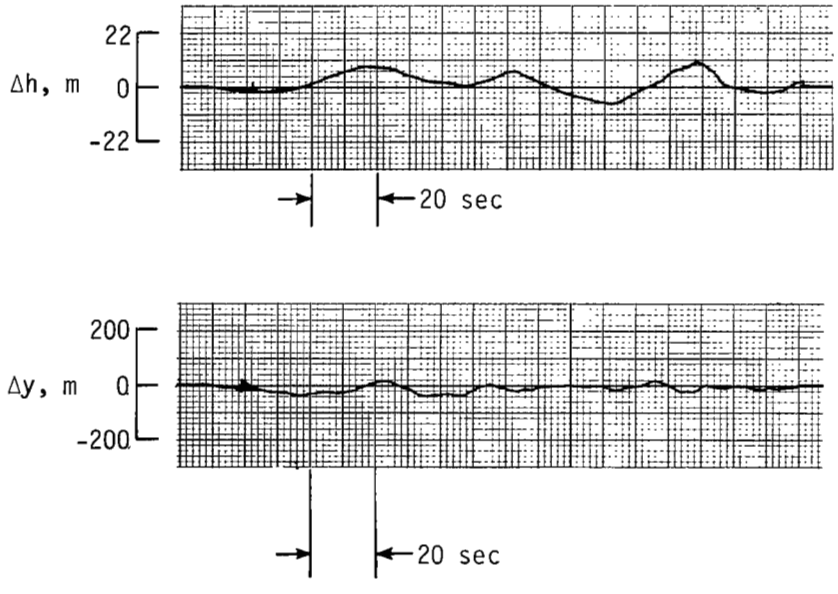

(c) Configuration 6.

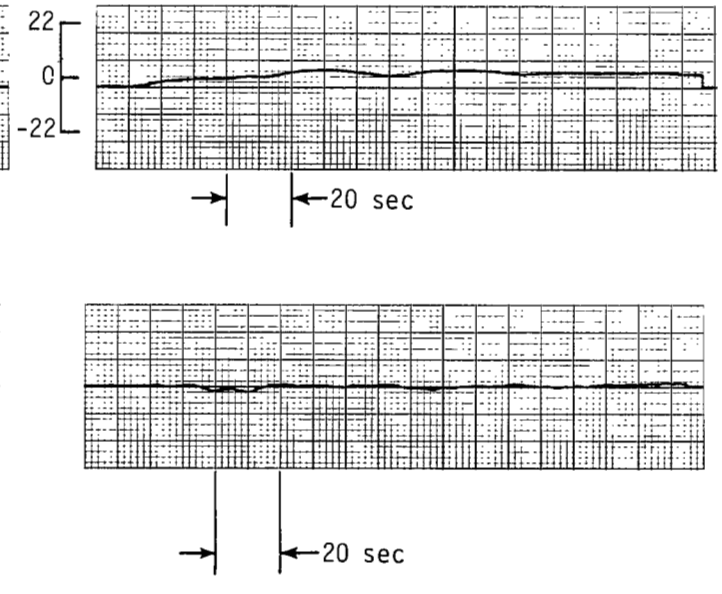

(d) Configuration 7.

Figure 6.- Sample time histories with turbulence for subject JS.

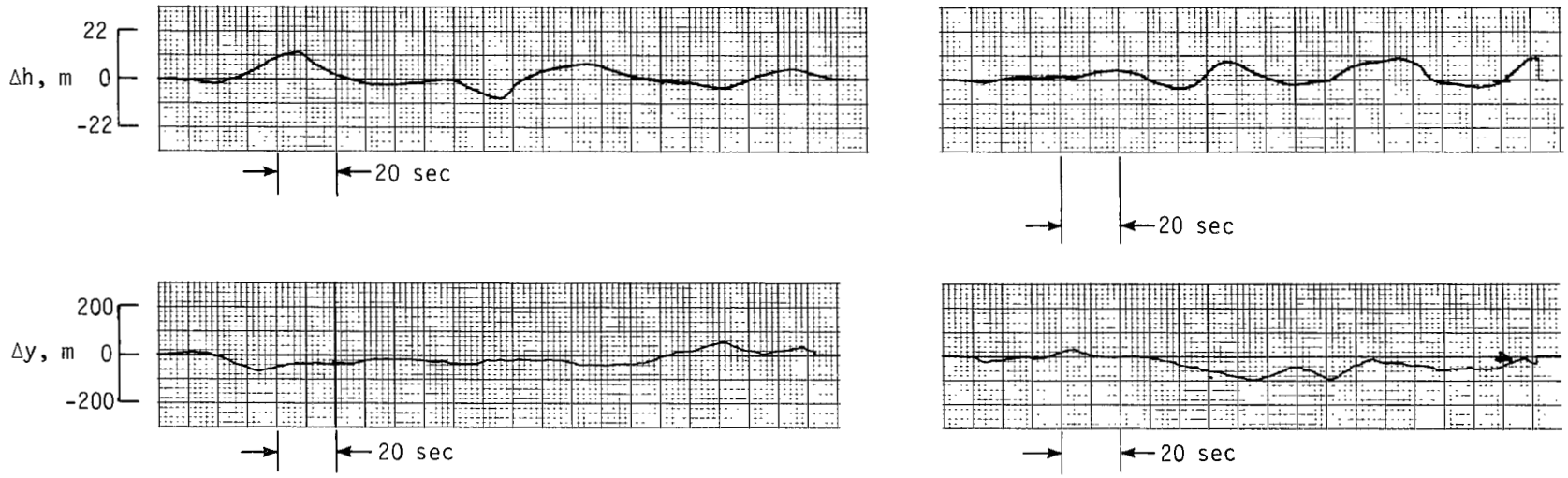

(a) Configuration 1.

(b) Configuration 5.

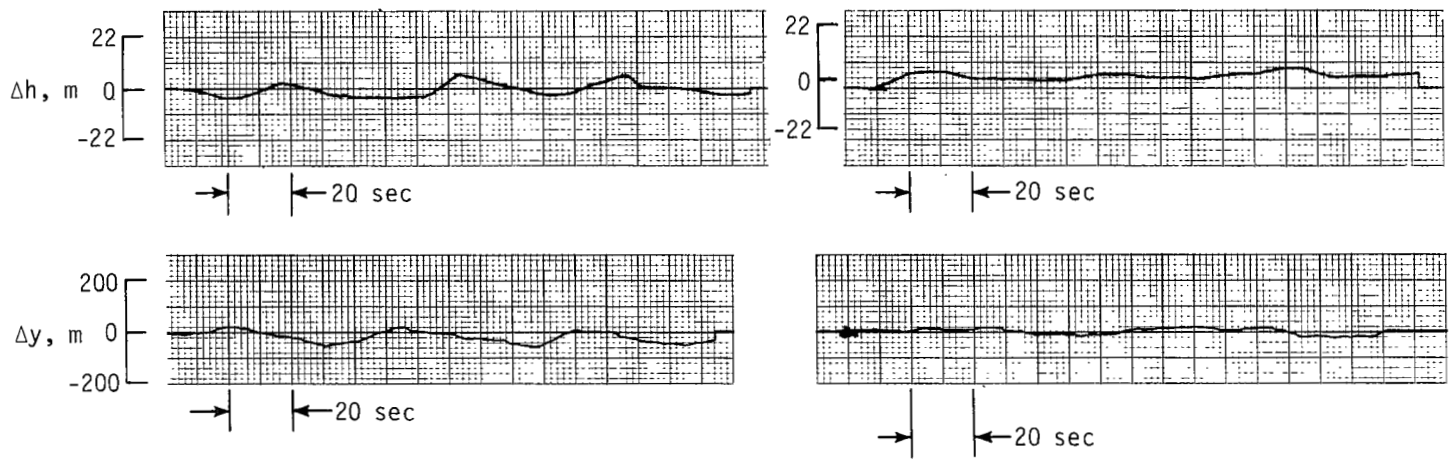

(c) Configuration 6.

(d) Configuration 7.

Figure 7.- Sample time histories with turbulence for subject DH.

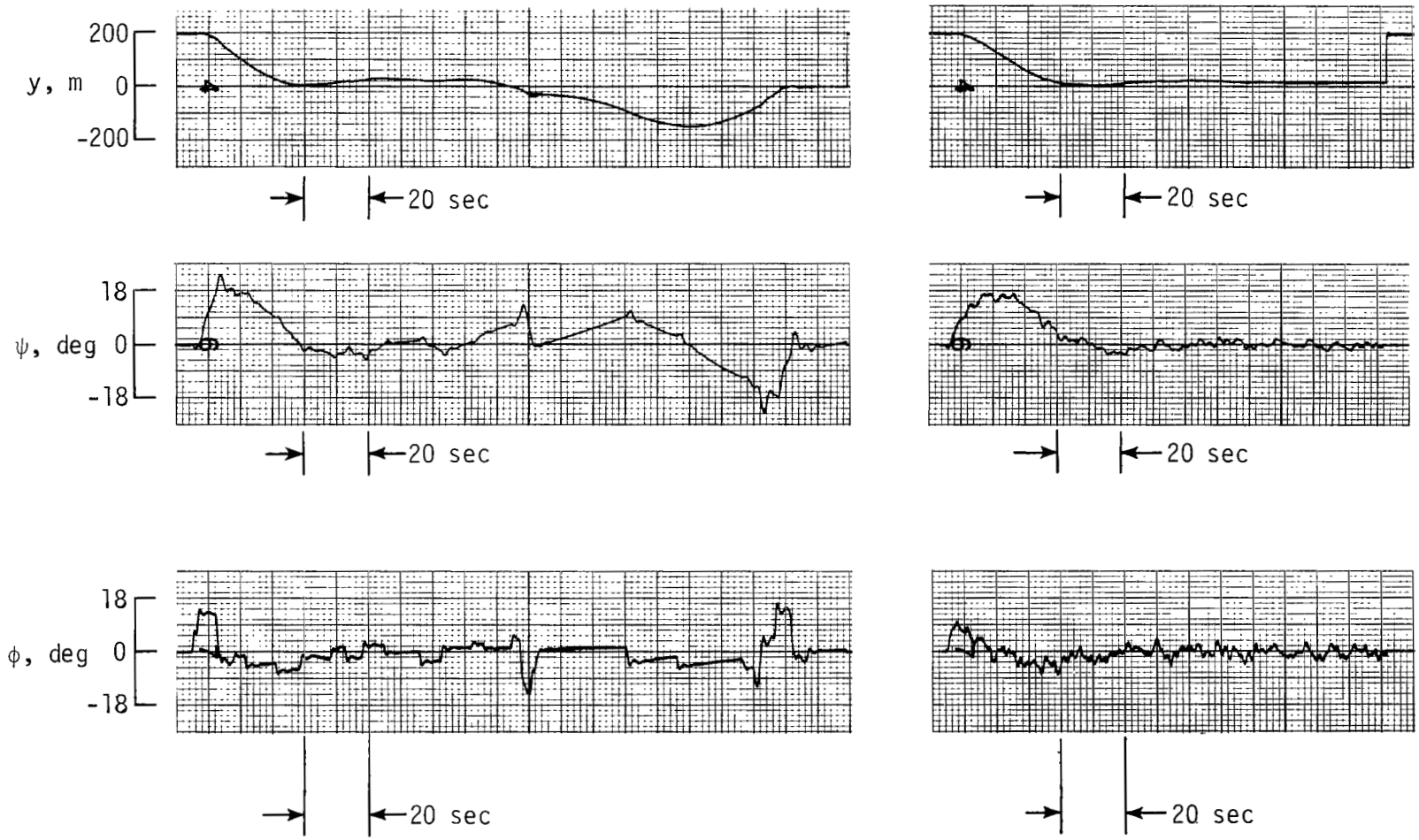

(a) Configuration 1.

Figure 8.- Step-input lateral response of subject WWA and corresponding pilot model.

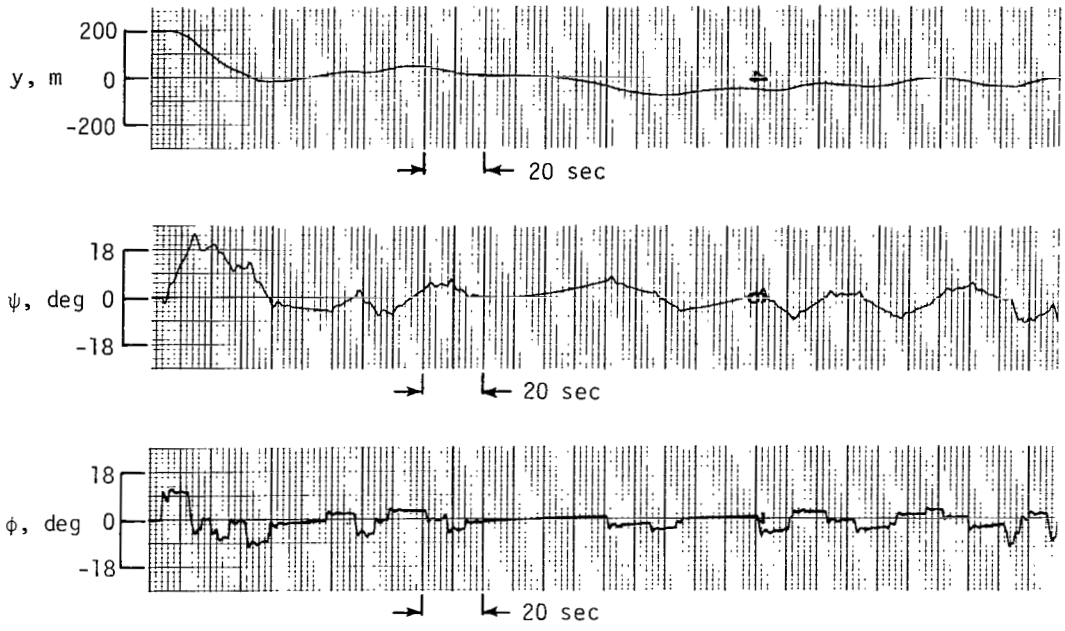

Subject

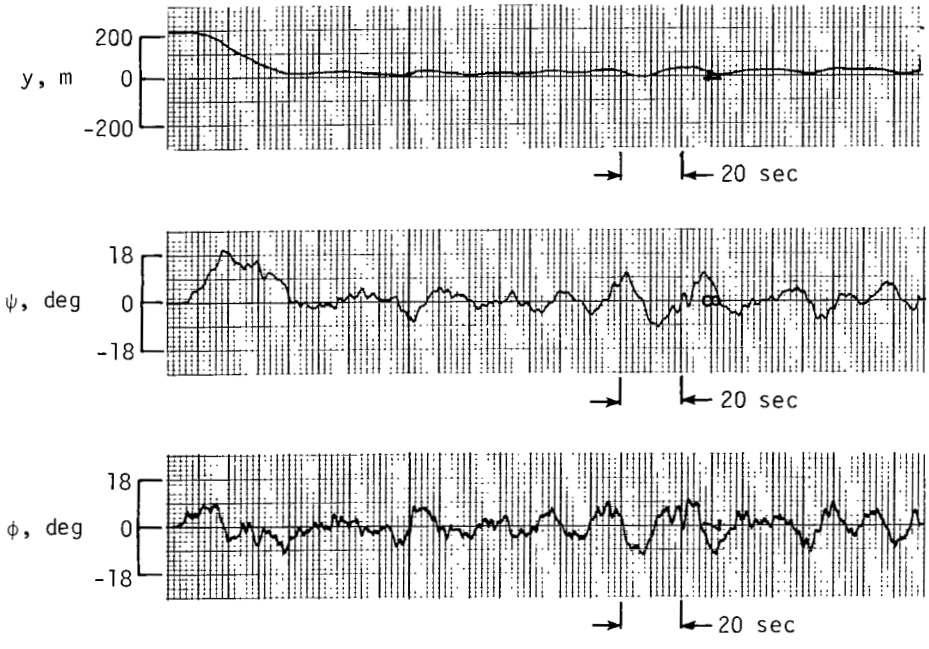

Model: K_{ϕ} = -0.47; K_{ψ} = 1.13; K_{y} = 0.00238 rad/m

(b) Configuration 5.

Figure 8.- Continued.

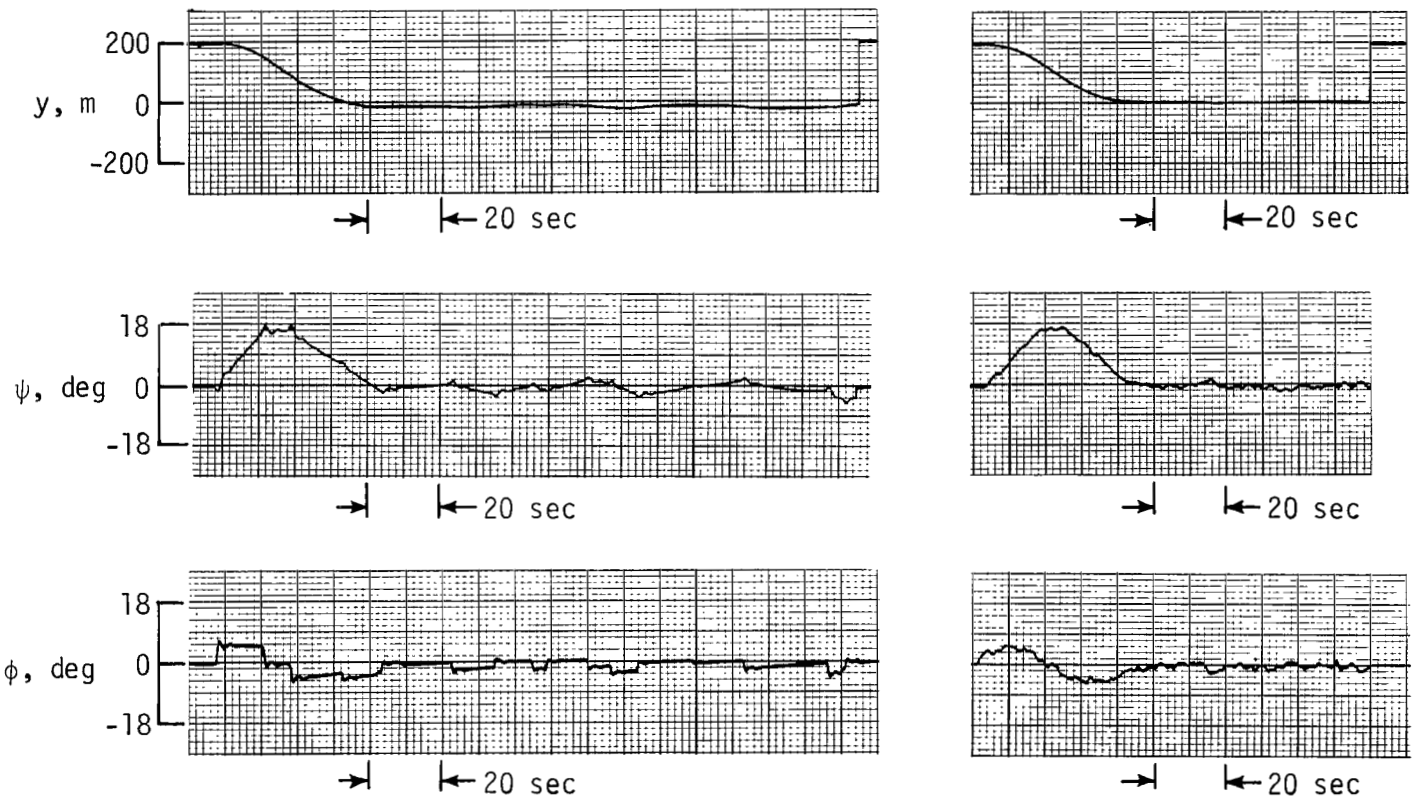

Subject

Model: K_{ϕ} = -0.75; K_{ψ} = 1.13;
K_{y} = 0.00138 rad/m

(c) Configuration 6.

Figure 8.- Continued.

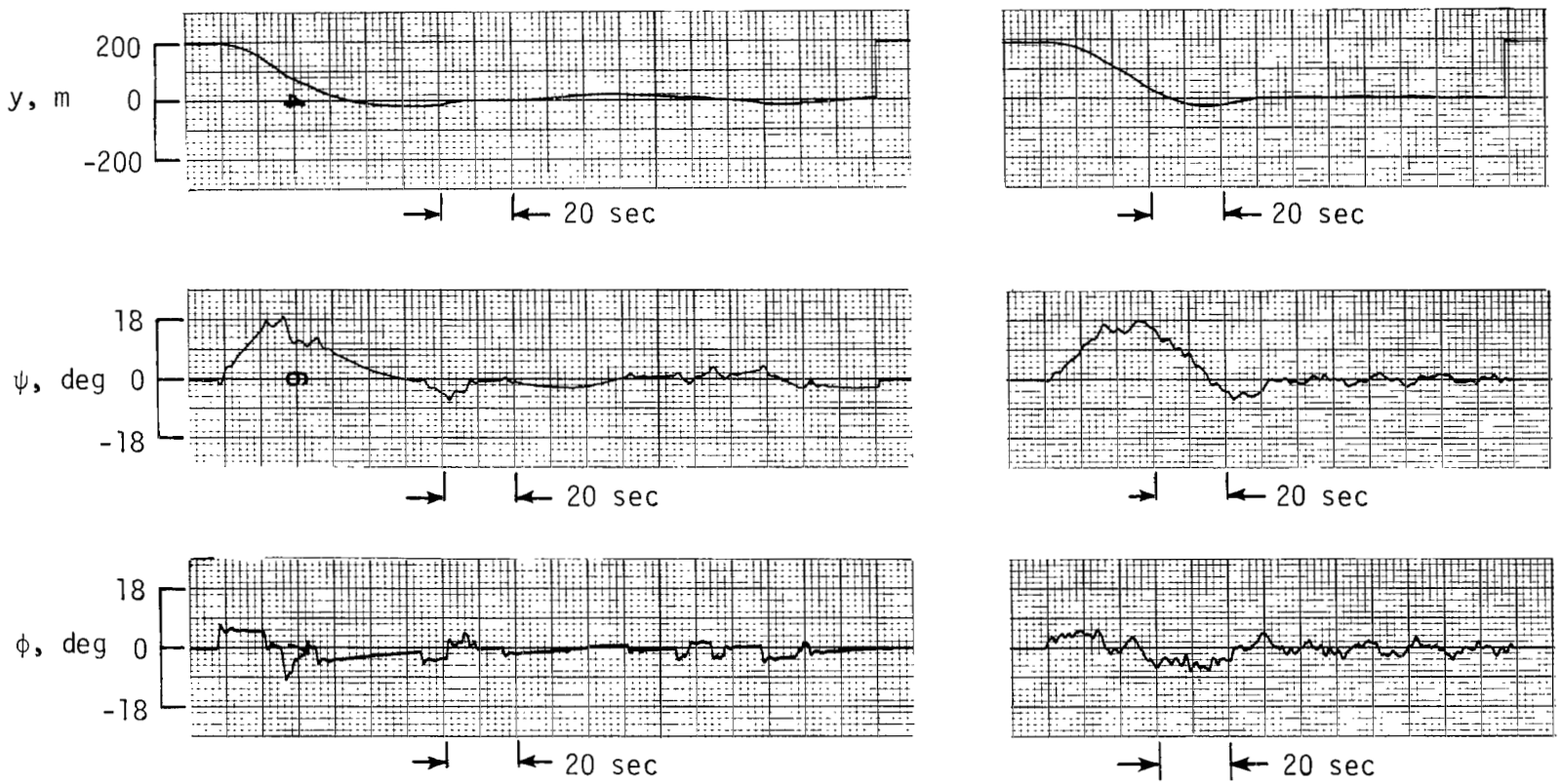

Subject

Model: $K_{\phi} = -0.75$; $K_{\psi} = 1.12$;

$K_y = 0.00186$ rad/m

(d) Configuration 7.

Figure 8.- Concluded.

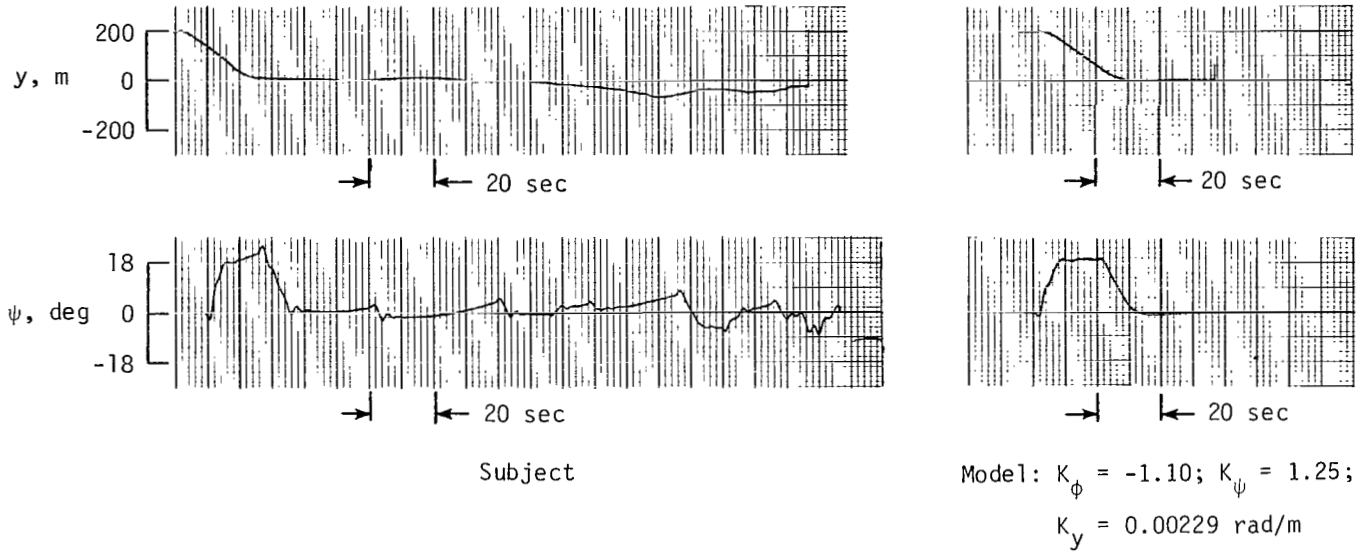

(a) Configuration 1.

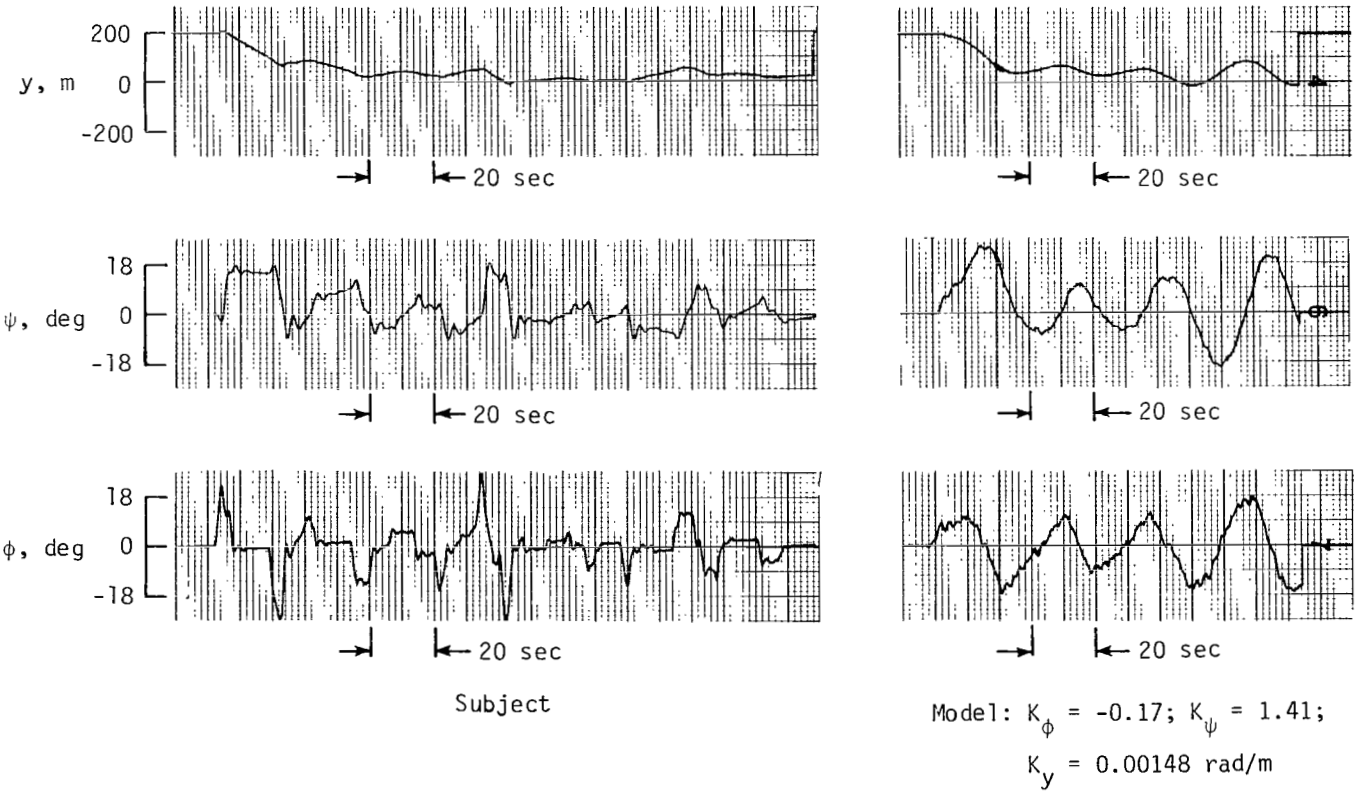

(b) Configuration 5.

Figure 9.- Step-input lateral response of subject MM and corresponding pilot model.

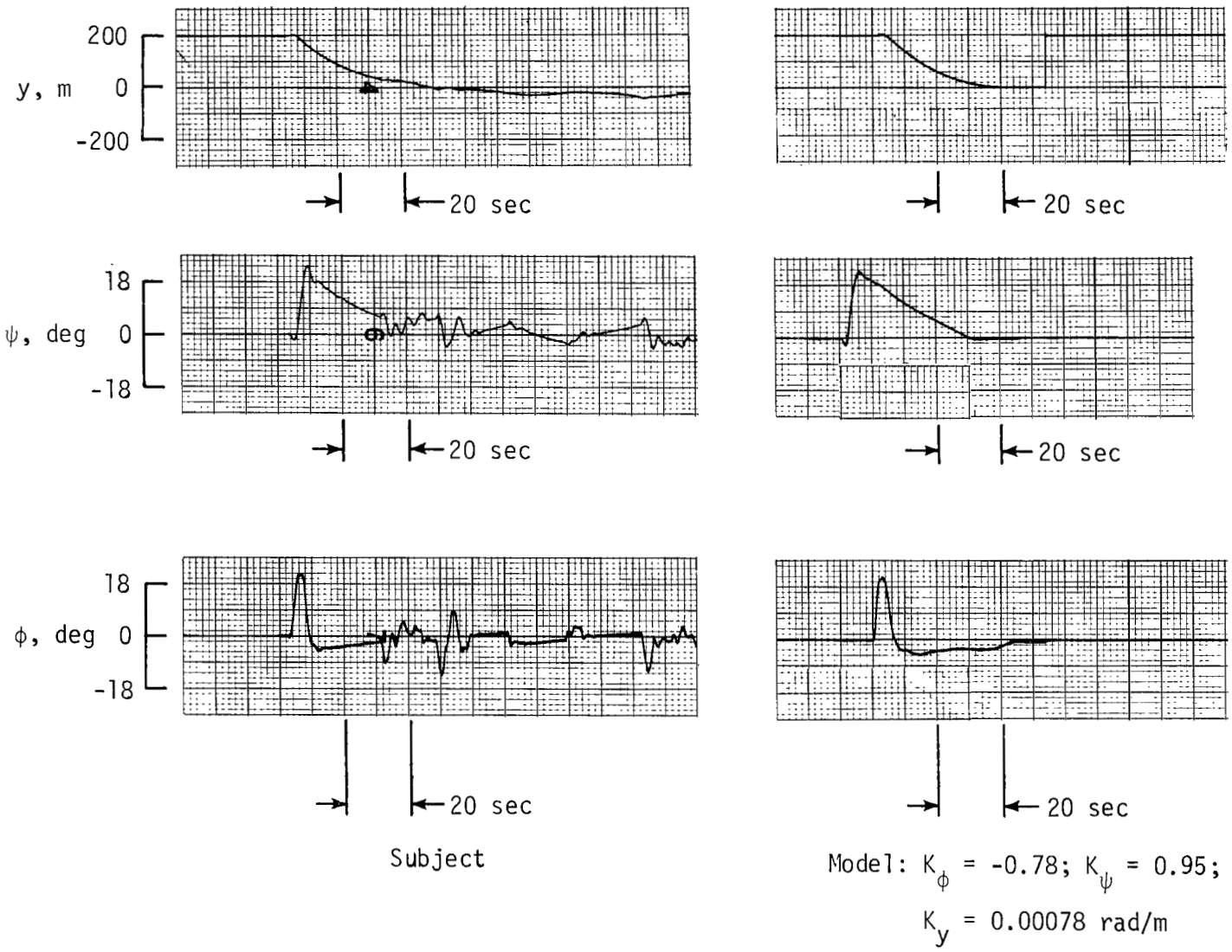

(c) Configuration 6.

Figure 9.- Continued.

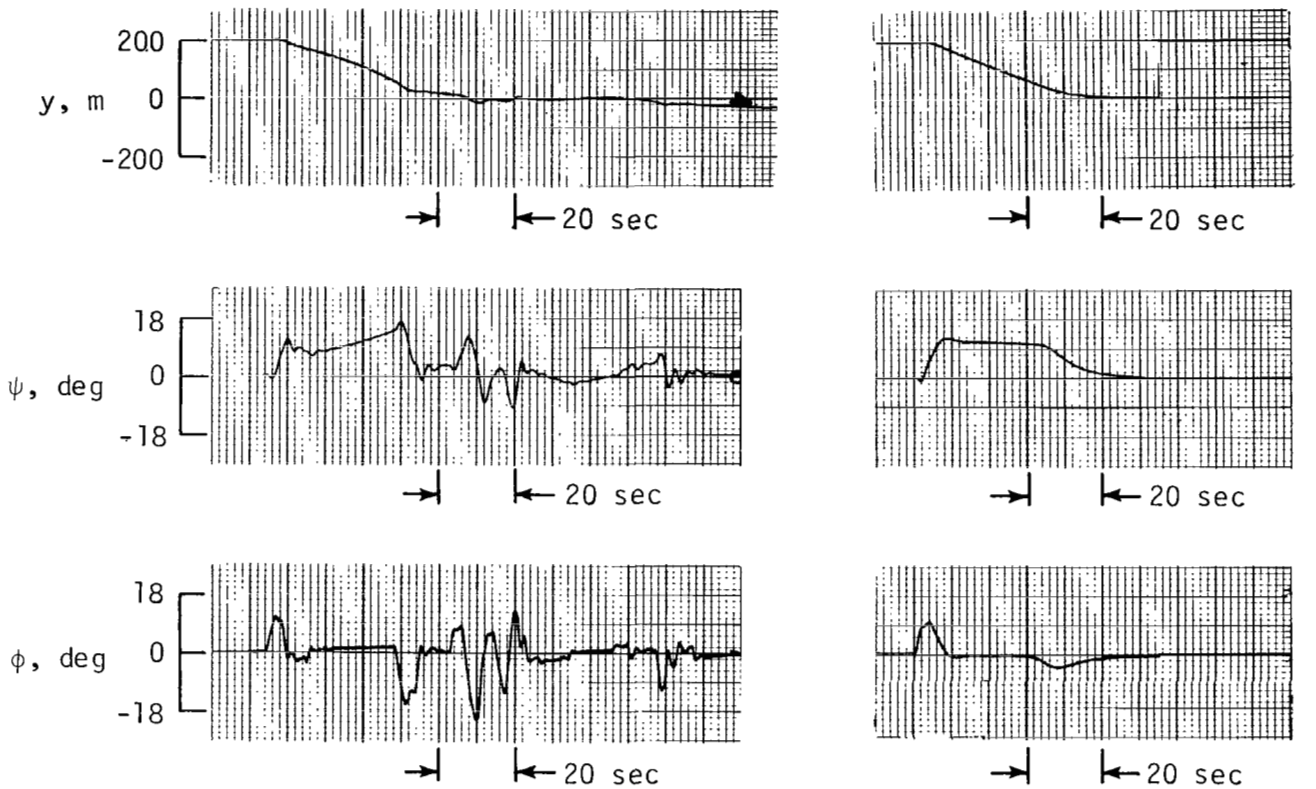

(d) Configuration 7.

Figure 9.- Concluded.

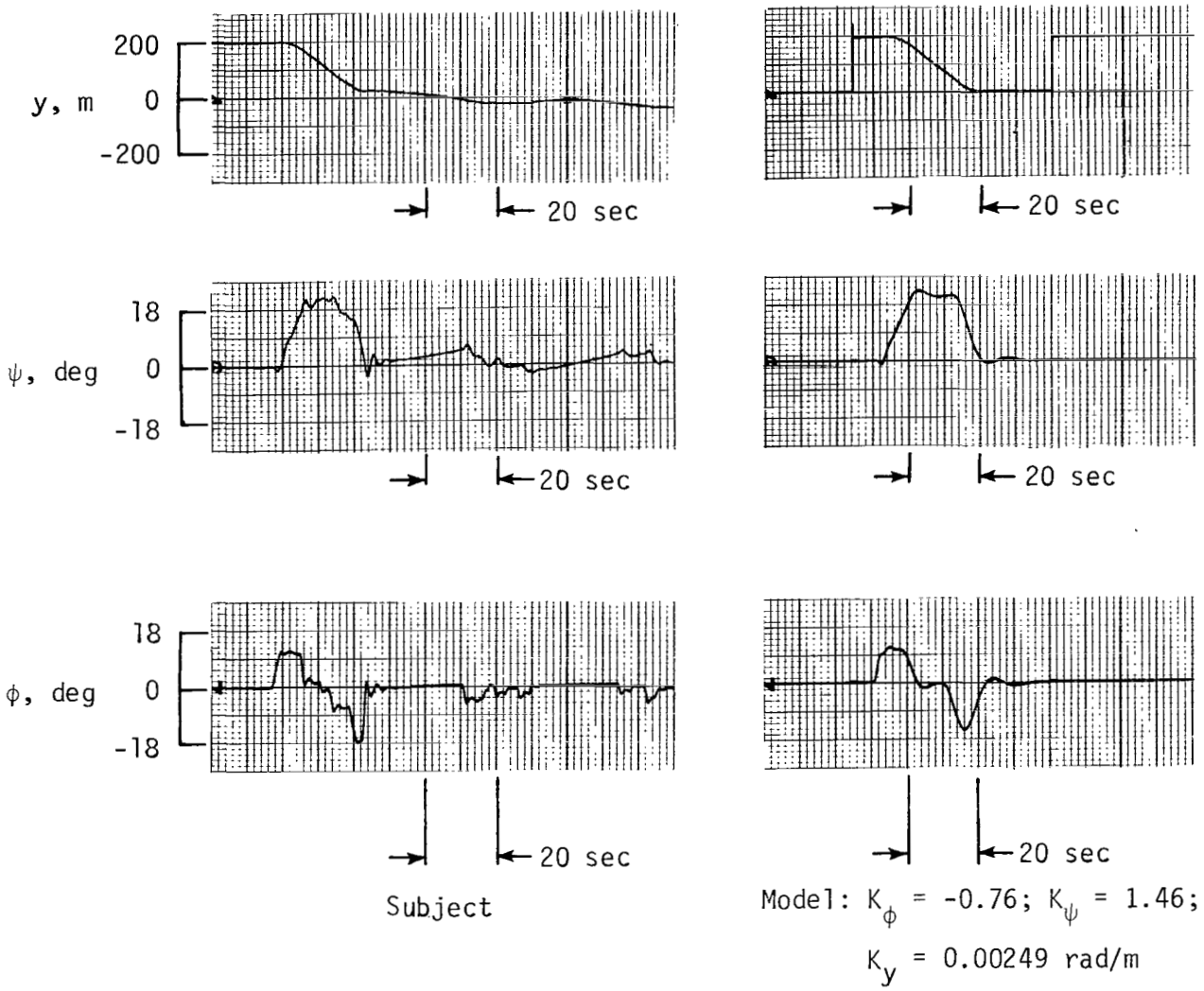

(a) Configuration 1.

Figure 10.- Step-input lateral response of subject CP and corresponding pilot model.

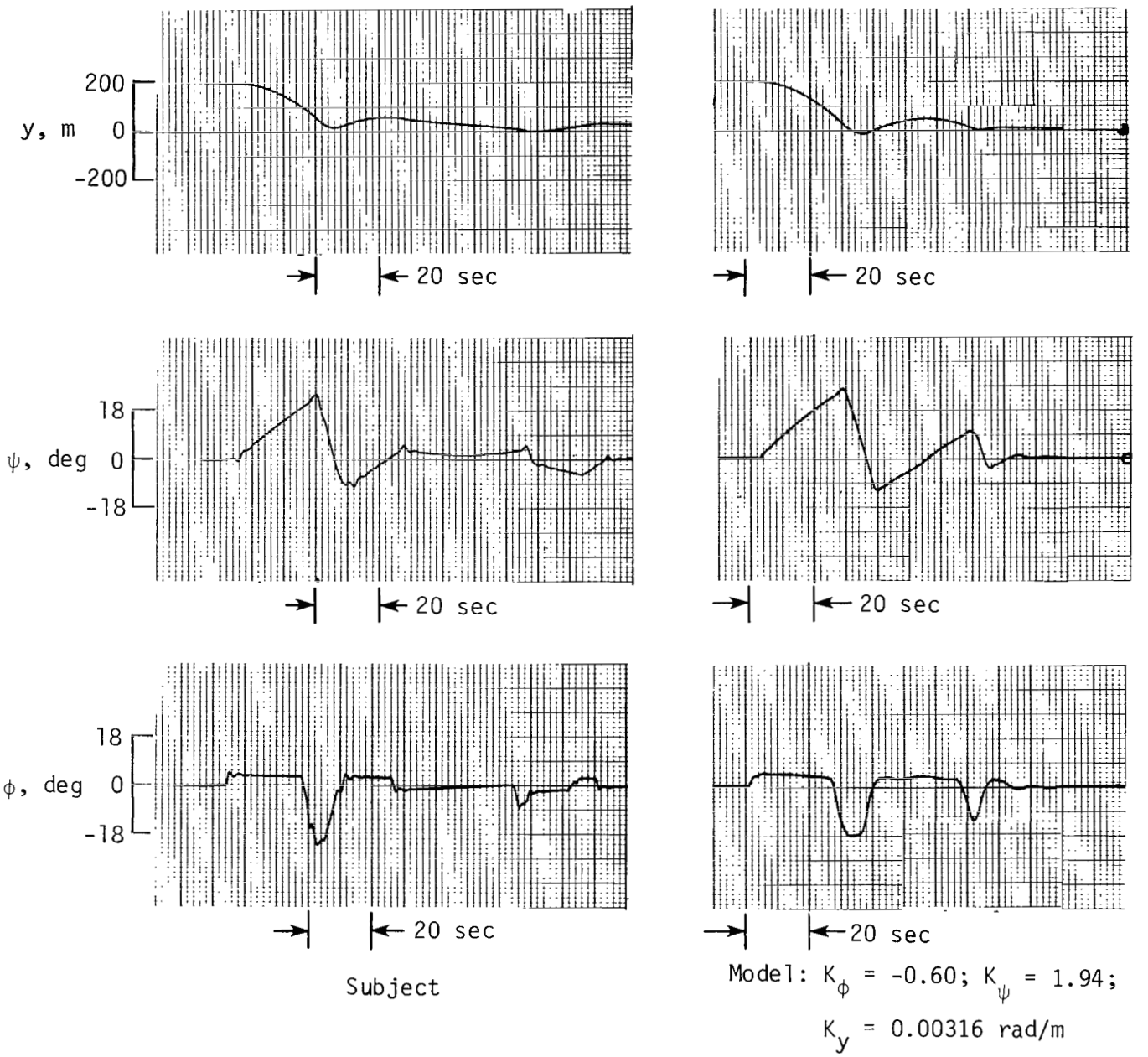

(b) Configuration 5.

Figure 10.- Continued.

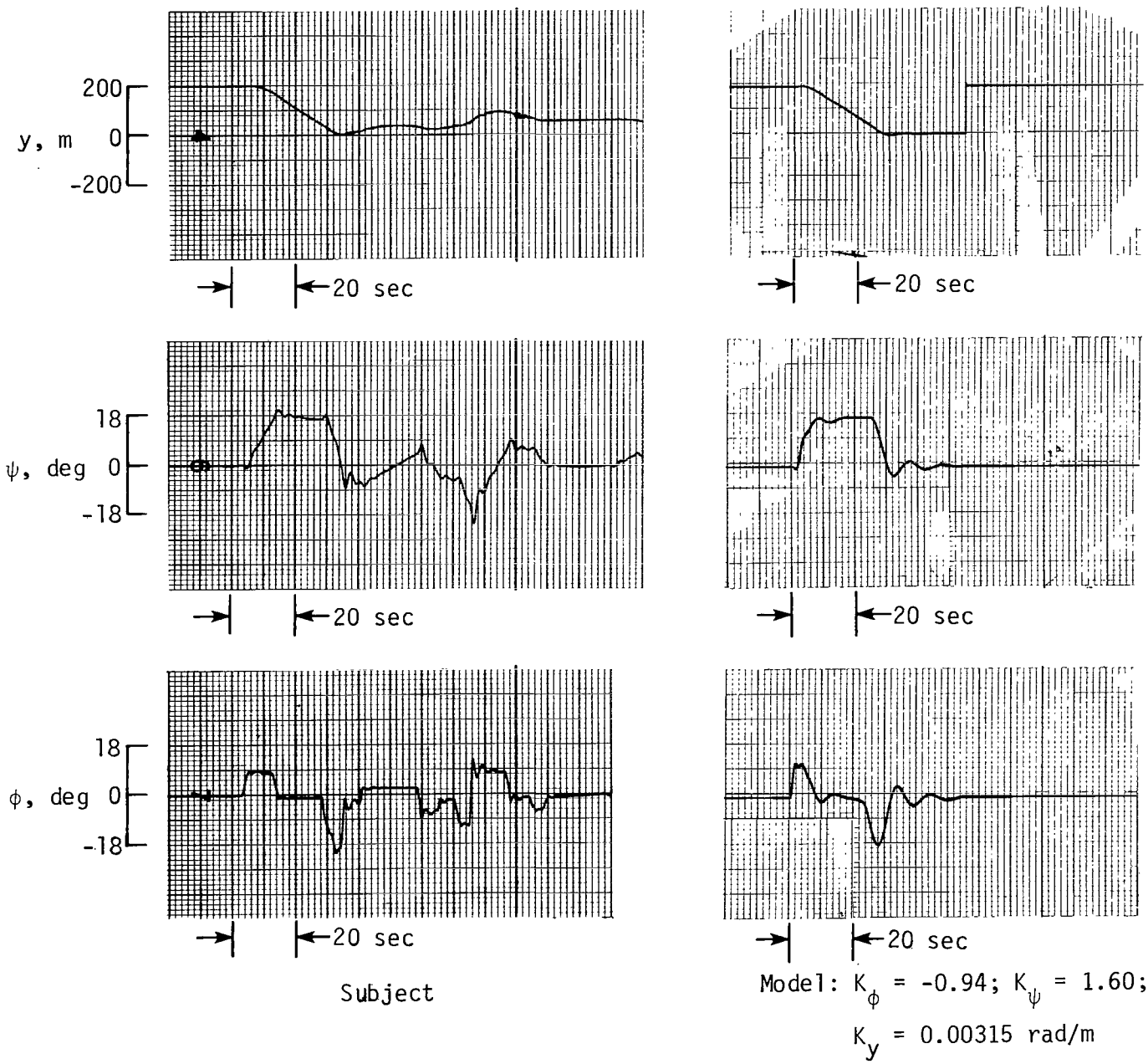

(c) Configuration 6.

Figure 10.- Continued.

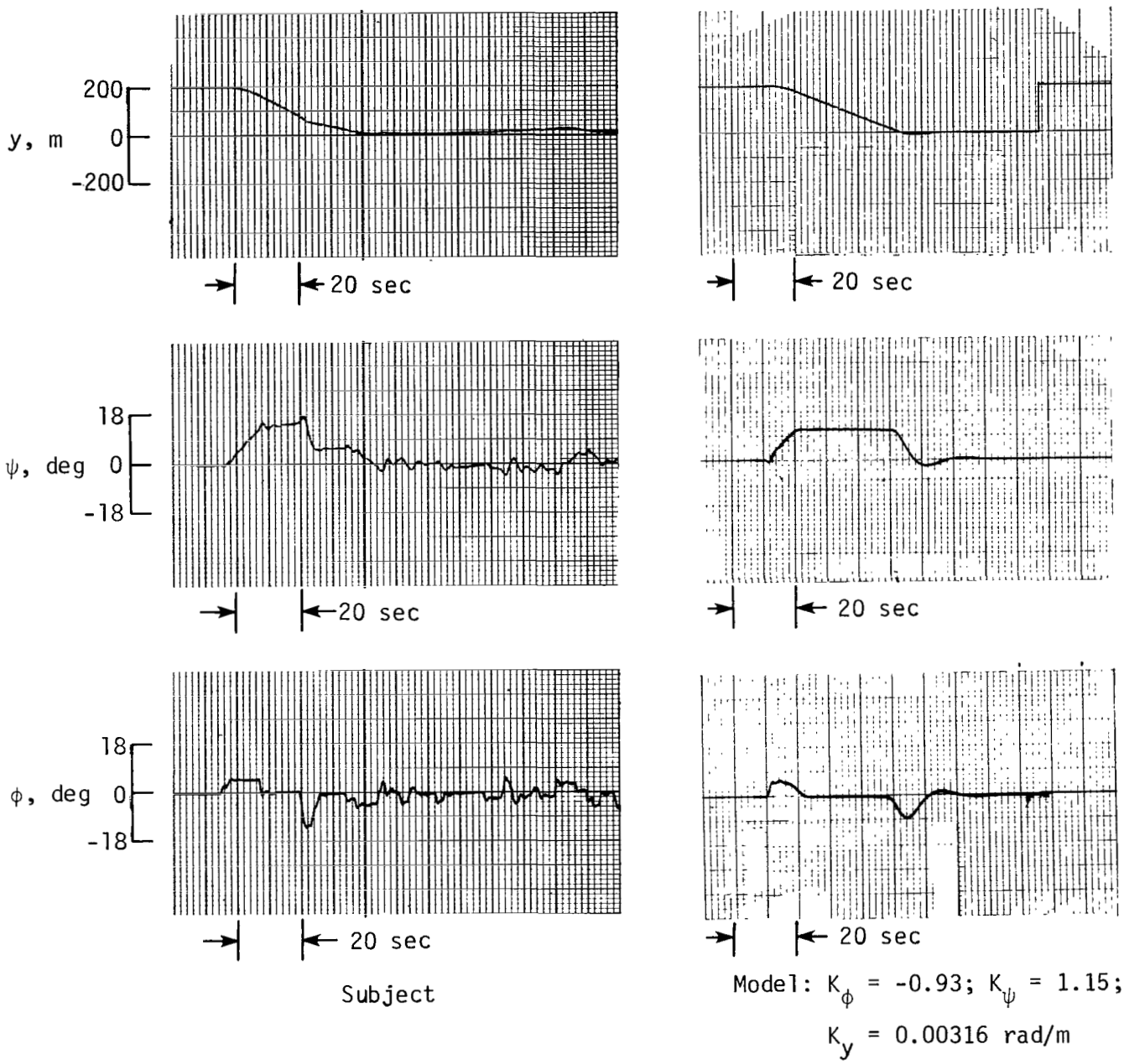

(d) Configuration 7.

Figure 10.- Concluded.

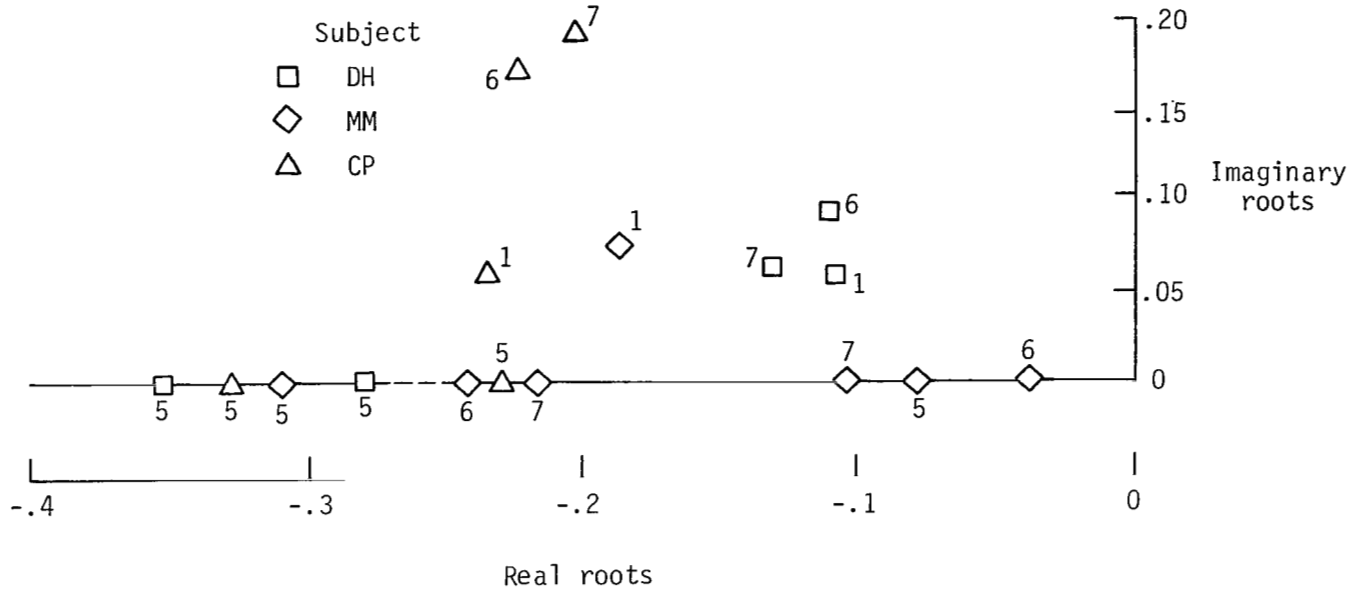

(a) y-mode roots.

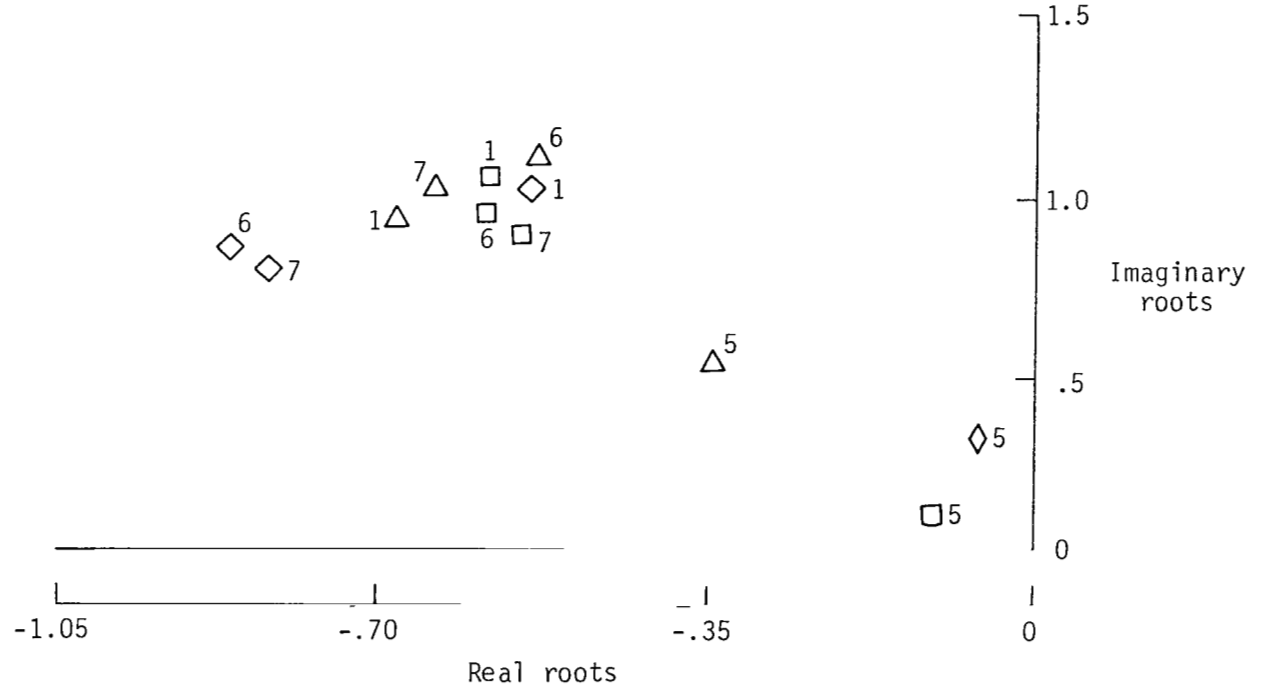

(b) Roll-heading angle mode roots.

Figure 11.- Disposition of closed-loop poles in different configurations. Numbers beside data symbols indicate configuration.

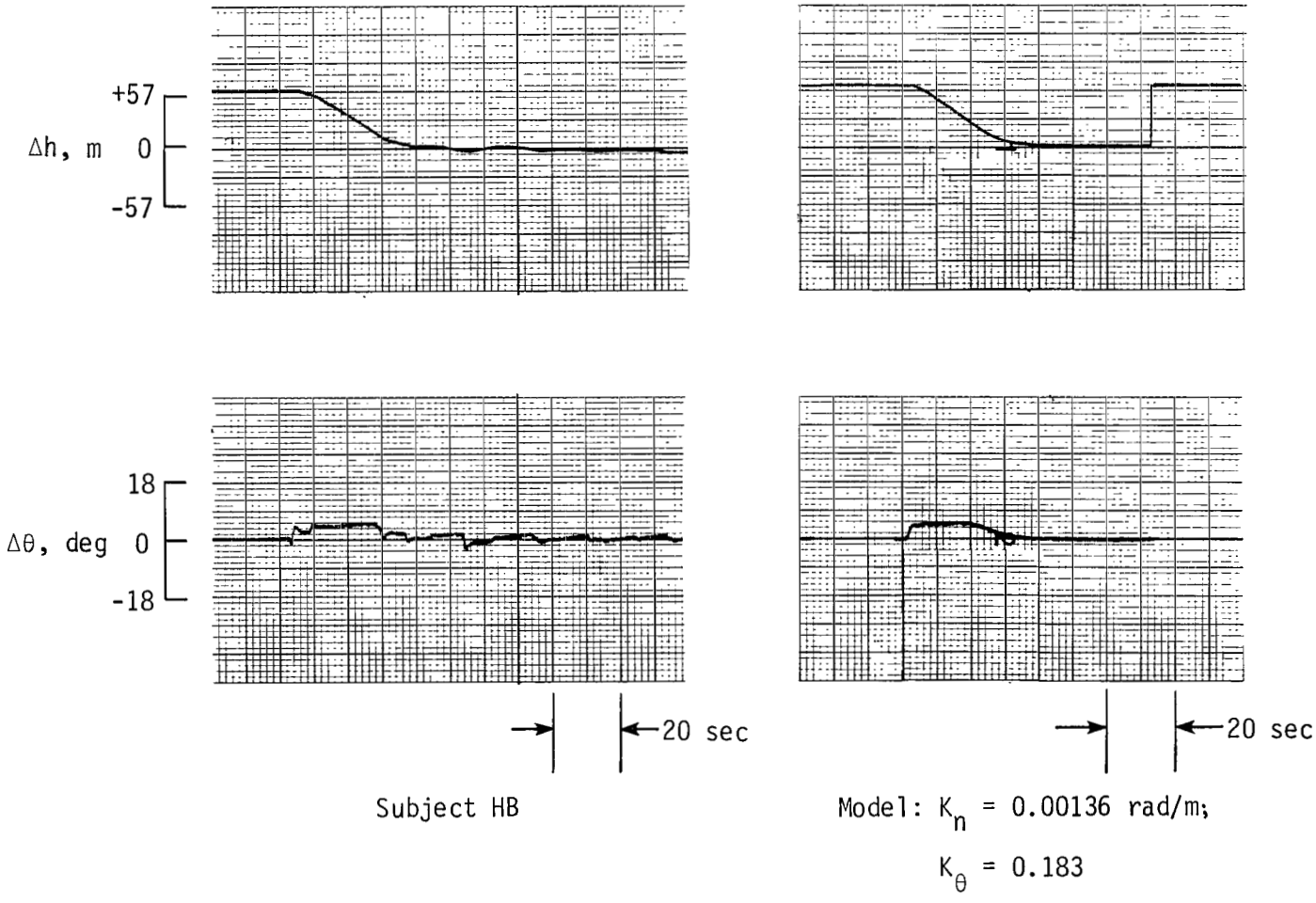

Figure 12.- Step-input response for vertical control with configuration 1.

1. Report No.	2. Government Accession No.	3. Recipient's Catalog No.
NASA TP-1915		

4. Title and Subtitle	5. Report Date
SIMULATOR EVALUATION OF SEPARATION OF DISPLAY PARAMETERS IN PATH-FOLLOWING TASKS	October 1981
	6. Performing Organization Code 505-41-73-04
7. Author(s)	8. Performing Organization Report No.
Garimella R. Sarma and James J. Adams	L-14590
	10. Work Unit No.
9. Performing Organization Name and Address	
NASA Langley Research Center Hampton, VA 23665	11. Contract or Grant No.
	13. Type of Report and Period Covered
12. Sponsoring Agency Name and Address	Technical Paper
National Aeronautics and Space Administration Washington, DC 20546	14. Sponsoring Agency Code

15. Supplementary Notes

Garimella R. Sarma: NRC-NASA Research Associate, now with National Aeronautical Laboratory, Bangalore, India.
James J. Adams: Langley Research Center.

16. Abstract

A five-degree-of-freedom, fixed-base simulation study was undertaken to examine the effect of changing the location of the displays for bank angle, pitch angle, heading angle, and the vertical and lateral displacement from an instrument landing system path. Analysis of the data obtained from eight subjects shows that the accuracy of the lateral path following and the pilot-aircraft system dynamic characteristics deteriorate when bank angle is displayed separated from the other attitudes. The best results were obtained when bank, heading, and pitch angles were displayed together and vertical and lateral displacements were displayed at another location in the display.

17. Key Words (Suggested by Author(s))	18. Distribution Statement
Aircraft display Pilot-induced oscillations Pilot models Lateral control	Unclassified - Unlimited Subject Category 06

19. Security Classif. (of this report)	20. Security Classif. (of this page)	21. No. of Pages	22. Price
Unclassified	Unclassified	42	A03

For sale by the National Technical Information Service, Springfield, Virginia 22161

NASA-Langley, 1981

National Aeronautics and
Space Administration

Washington, D.C.
20546

Official Business
Penalty for Private Use, $300

THIRD-CLASS BULK RATE

Postage and Fees Paid
National Aeronautics and
Space Administration
NASA-451

U.S.MAIL

I I IU,A, 100881 S00903DS
DEPT OF THE AIR FORCE
AF WEAPONS LABORATORY
ATTN: TECHNICAL LIBRARY (SUL)
KIRTLAND AFB NM 87117

NASA

POSTMASTER: If Undeliverable (Section 158 Postal Manual) Do Not Return